The 3D nuclear organization of telomeres during endometrial carcinoma development

By

Adrian Danescu

A Thesis submitted to the Faculty of Graduate Studies of

The University of Manitoba

in partial fulfilment of the requirements of the degree of

MASTER OF SCIENCE

Department of Human Anatomy and Cell Science

Faculty of Medicine

University of Manitoba

Winnipeg

ABSTRACT

Early diagnosis of endometrial cancer (EC) is uncertain and women undergo preventive hysterectomy in cases where a non-invasive treatment can be used instead.

To contribute to solving this challenge we investigated if early changes in the nuclear 3D telomere architecture during carcinoma development can be detected prior to the first morphological evidence of precancerous lesions. We utilized Pten heterozygous mice that develop progressive carcinoma in the endometrial tissue similar to EC development in women. We used telomere fluorescence in situ hybridization (FISH), 3D molecular imaging and analysis techniques on interphase nuclei of endometrial glandular epithelial cells to identify alterations in the 3D-telomere profile. We found that telomere dysfunction in Pten heterozygous mice is present already in endometrial simple hyperplasia lesions prior to detectable loss of PTEN protein expression and that the 3D telomere architecture has a specific signature that indicates early telomere dysfunction predictive for endometrial malignant transformation.

ACKNOWLEDGEMENTS

I want to thank my wife for her love, motivation and support during my research years.

I express much appreciation to my supervisor Dr. Sabine Hombach-Klonisch for the extraordinary help and guidance during my graduate study endeavor. All my lab techniques, critical thinking, scientific reading and writing skills have been improved considerably because of your suggestions!

Special thanks to Dr. Sabine Mai for training and mentoring me during my project.

Also, I want to thank my committee members, Drs. J. Elliott Scott and Louise Simard.

This work was made possible due to the collaboration with Dr. Antonio DiCristofano. Thank you!

Further, I appreciate the support from Department Head, Dr. Tomas Klonisch and the entire Department of Human Anatomy and Cell Science.

My gratitude goes also to Mary Cheang for helping me with the statistical analysis and Landon Wark who provided me with valuable information to interpret my results.

I thank all the lab members for their help and positive attitude that made the days in the lab enjoyable.

The financial support for this project was provided by: NSERC, MHRC and CIHR- ITMHRT.

TABLE OF CONTENTS

LIST OF TABLES

LIST OF FIGURES

LIST OF ABBREVIATIONS

(2D) two dimensional

(3D) three dimensional

(ABC) avidin/biotin blocking

(AH) atypical hyperplasia

(ALT) alternative lengthening of telomere

(ATM) ataxia telangiectasia mutated

(ATR) ataxia telangiectasia and Rad3-related

(BFB) breakage fusion bridge

(CCDs) Charge Coupled Devices

(CAH) complex atypical hyperplasia

(CH) complex hyperplasia

(Chk1) cell cycle checkpoint kinase

(CTs) chromosome territories

(DAB) 3,3'-diaminobenzidine

(DAPI) 4',6-diamino-2-phenylindole

(DNA) deoxyribonucleic acid

(DSB) double strand breaks

(EC) endometrial carcinoma

(ER) estrogen receptor

(ERα) estrogen receptor alpha

(ER β) estrogen receptor beta

(ES) embryonic stem cells

(E2) estrogen

(FISH) Fluorescence in situ hybridization

(H&E) hematoxylin and eosin

(HRP) horseradish peroxidase

(IgG) immunoglobulin G

(LOH) loss of heterozygosity

(MI) microsatellite instability

(mRNA) messenger ribonucleic acid

(NaSCN) sodium thiocyanate

(PI3K) phosphatidylinositol 3-kinase

(PIP3) phosphatidyl-inositol 3,4,5 triphosphate

(PNA) peptide nucleic acid

(POT1) protection of telomeres 1

(PR) progesterone receptor

(PSF) point spread function

(PTEN) phosphatase and tensin homolog deleted on chromosome ten

(RAP1) repressor or activator protein 1

(RNA) ribonucleic acid

(SH) simple hyperplasia

(SSC) saline-sodium citrate

(TA) telomere aggregates

(TBS) Tris-Buffered Saline

(TBST) Tris-Buffered Saline Tween

(TIN2) TRF1 and interacting nuclear protein 2

(T-loop) telomere loop

(TPP1) POT1 and TIN2 interacting protein

(TRF1) telomeric repeat binding factor 1

(TRF2) telomeric repeat binding factor 2

(WHO) World Health Organization

(WT) wild type

Chapter I: INTRODUCTION

Our investigation in the present study is focused on the identification of changes in the 3D telomere profiles during endometrial carcinoma development, especially in the early stages.

The diagnosis of endometrial precancerous lesions involves a certain degree of uncertainty for pathologists and gynecologists and because of this uncertainty, some women are advised to undergo hysterectomy as a preventive measure. Our study is based on new tools and methods that allow us to focus on the changes in the nuclear 3D telomere architecture during the development of endometrial carcinoma, especially prior to the first morphological evidence of precancerous lesions. We are using Pten heterozygous mouse to model type-I endometrial carcinoma development in humans.

With the following paragraphs, I will provide an introduction and overview about endometrial carcinoma and the role of PTEN, the structure and function of telomeres, and the fluorescent imaging method we have used.

I. ENDOMETRIAL CARCINOMA

Endometrial carcinoma is a common malignancy of the female reproductive tract localized in the uterus. In the US, in 2010, more than 40, 000 new cases of endometrial carcinoma were diagnosed and almost 8, 000 women died from this type of cancer [1]. Endometrial carcinoma was shown to be caused by the accumulation of genetic

alterations. Among the most commonly altered genes in this type of cancer are: PTEN, p53, K-ras, β-catenin, Her-2/neu [2-5].

Endometrial carcinoma has a higher survival rate when compared with other types of cancer (85% at 5 years) but the potential malignant transformation of endometrial precancerous lesions generates also a high morbidity rate [5-7]. In order to avoid the risk of malignancy, hormone therapy with progestin (anti-estrogenic effect) or hysterectomies are chosen as optimal solutions [5, 8].

To elucidate the molecular events involved in the development of endometrial carcinoma in humans, mouse models mimicking this pathology have been created in the last decades [9-11].

1. Human Endometrium

The endometrium is the inner lining of the uterus and consists of luminal epithelium, glandular epithelium, stroma, blood vessels and immune cells [12]. Functionally, the endometrium is separated into two layers: a functional layer which is closer to the lumen and a basal layer closer to the myometrium. Estrogen and progesterone hormones differentially stimulate the endometrium and remodel it during a three stage cycle [13, 14]. During the secretory stage the levels of progesterone, predominantly secreted by the corpus luteum, increase. If embryo implantation does not occur, the functional layer is shed during menstruation. Menstruation is the process whereby the upper two thirds of the endometrium (functional layer) are shed and regenerated on a repetitive basis under the influence of estrogen produced by the ovarian granulosa and

theca interna cells (follicular stage). The endometrium regenerates from the basal layer [15]. The action of the steroid hormones is mediated by specific receptors for estrogen and progesterone through which they regulate transcriptional activities. There are two subtypes for both receptors: estrogen receptors (ER)(ERα and ER β) [16] and progesterone receptors (PR)(PR-A and PR-B) [17]. ERα is expressed in pre-menopausal endometrium by glandular and stromal cells during the proliferative phase and, ERα decreases during the secretory phase [18]. The endometrial expression of ER and PR is a fine balance during the menstrual cycle [19]. Both estrogen and progesterone have an important role in regulating the expression of ER and PR; during the proliferative stage estrogen up-regulates ER and PR and, during the secretory stage, progesterone down-regulates them [20]. Estrogen stimulates endometrial proliferation [21] , but, once the PR becomes active in the secretory stage, this proliferation decreases.

In older women, when the endometrial cycle ceases after menopause, the endometrium will become atrophic with a decreased number of glands scattered in the stroma. Menopause is “the final period or menses occurring after natural depletion of ovarian follicles or from damage to or removal of the ovaries” [22].

When ER expression is unbalanced (excess ER and insufficient PR), the endometrium is more sensitive to estrogenic action and estrogen-related endometrial hyperplasia and carcinoma can develop [23]. Endometrial hyperplasia can be reversible in many cases or it can progress to complex atypical hyperplasia in other cases. In approximately 25% to 30% of atypical hyperplasia, there is a risk of progressing to endometrial carcinoma

[8, 24]. During endometrial carcinoma development, different types of tissue changes can be seen ranging from non-malignant stages to fully invasive carcinomas [25-28] . When compared to other types of cancer, endometrial cancer is more complex because the variability in precancerous lesions making the diagnosis more challenging [29-31].

Based on pathology, two major types of endometrial cancer were described: endometrioid (type I) and non-endometrioid (type II) [32, 33]. The type I endometrial carcinoma is an estrogen-related carcinoma, and develops from endometrial hyperplasia (endometrioid histology). The type II endometrial carcinoma is not estrogen-related, and presents different histological types, particularly serous carcinomas and clear-cell carcinomas. Type II carcinoma has a poor prognosis when compared with type I [34, 35]. A dualistic model of endometrial carcinogenesis was proposed based on two different pathogenetic pathways of endometrial carcinoma [36].

2. Endometrial Hyperplasia

Endometrial hyperplasia is a benign proliferation of the endometrium that histologically presents an increase of the number of glands with a variable gland shape and gland size [37].

The endometrial hyperplasia can be simple (SH), or complex with or without atypia (CH) or (CAH); the glandular tissue architecture differentiates between them [8, 38]. SH is characterized by a close to normal gland to stroma ratio, glands with irregular size but cell polarity is not affected (the cells orient themselves to the basal membrane)[8]. CH is defined by irregular glands and an increased gland to stroma ratio in contrast with the

CAH that have atypical nuclei (increase in nuclear size and change in chromatin distribution) and loss of cell polarity (cells cannot orient themselves in apical or basal direction) [8, 39].

Gynecologists and pathologists encounter difficulties in diagnosing the different histological types of endometrial hyperplasia in the human mainly because the diagnostic criteria established by the WHO are in some cases subjective [40, 41]. Computerized morphometric analysis and molecular genetics classification were introduced as a possible solution for the diagnostic of endometrial carcinoma precursors [41]. Based on the diagnosis, hyperplastic lesions require different treatments. In atypical hyperplasia treatment with progestin in high doses is recommended, especially for young women, where surgical procedures are not attractive. In contrast, similar conditions in older women are treated surgically by hysterectomy [42].

3. Endometrioid Carcinoma

Endometrioid carcinoma covers 80% of the cases of endometrial carcinoma and it was shown to be related with the unopposed estrogen stimulation in the endometrium [5] for which obesity and diabetes are among the major causes. Specific genetic changes such as mutations in the PTEN gene and microsatellite instability (MI) differentiate the endometrioid carcinoma from other endometrial carcinoma subtypes [43]. PTEN mutations were shown to have an early contribution in this type of cancer by altering normal cell growth, apoptosis and migration [44]. Microsatellite instability (MI) with minor genetic alterations and K-ras protooncogene mutations may also play a role in the

endometrioid cancer development [44-46]. The activation of the APC/beta-catenin/Tcf signaling pathway was associated as well in the development of endometrioid carcinoma [47]. In advanced stages of endometrioid carcinomas, p53 mutations and Her2/neu over expression were seen more frequently [48].

4. Non-Endometrioid Carcinoma

In contrast to the tumors dependent on unopposed estrogen influence, non-endometrioid endometrial carcinomas that originate from an atrophic endometrium may develop in postmenopausal women [32, 33]. Two of the most common forms of non-endometrioid carcinomas, clear cell carcinoma and serous papillary carcinoma, have a poor prognosis when compared with the endometrioid tumors [49].

5. PTEN Biology and Function

Loss of the tumor suppressor PTEN (phosphatase and tensin homolog deleted on chromosome ten) was shown to be an early marker for the transformation of glandular hyperplasia in type I carcinoma in the endometrium [44]. PTEN is a tumor suppressor commonly inactivated in various forms of cancers (such as prostate, breast, brain, endometrium) and was identified under the names of PTEN/MMAC1/TEP1 [9, 50-52]. PTEN genetic alterations are present in approximately 44% of glioblastomas [53], 50% of endometrial carcinomas [54] and 43% of prostate cancers [55]. The inactivation of PTEN can occur through: mutations, loss of heterozygosity (LOH) (loss of function of the remaining allele) or promoter methylation (methylation of the promoter region that leads to loss of gene function) [56, 57]. PTEN encodes a key protein of the

PTEN/phosphatidylinositol 3-kinase (PI3K)/AKT regulatory pathway [58]. This signaling pathway has significant functions in processes such as apoptosis, cell metabolism, cell proliferation and cell growth [58-61]. PTEN is a dual protein and lipid phosphatase. The lipid phosphatase activity of PTEN uses phosphatidyl-inositol 3,4,5 triphosphate (PIP3) as a substrate. An increase in PIP3 results in AKT activation [58-61]. By negatively regulating the AKT pathway, PTEN inhibits cell proliferation, cell growth and apoptosis [58, 59, 61].

6. PTEN and the Genome

One of the substrates phosphorylated by AKT is cell cycle checkpoint kinase (Chk1). This kinase has an important role in maintaining the stability of the genome by controlling the cell cycle timing that facilitates DNA repair and also by inducing the apoptosis of damaged cells [62]. Loss of PTEN was shown to lead to the ubiquitination of the Chk1 kinase in the cytoplasm and subsequent proteasomal degradation [63]. When Chk1 function is reduced due to PTEN loss, the mechanisms of DNA maintenance are compromised and DNA double strand breaks (DSB) cannot be repaired [64]. Consequently, the inhibition of Chk1 can generate abnormal chromosomes and genomic instability. PTEN can also control the integrity of chromosomes by physical association with the centromeres; it was shown that loss of PTEN leads to “centromere breakage and chromosomal translocations” [65]. Thus PTEN loss generates genomic instability. In addition, the interaction between PTEN and chromatin plays a role in DSB regulation by controlling Rad51, the homologous recombination repair pathway [65].

7. PTEN and Endometrial Carcinoma

PTEN is the most commonly altered gene in endometrial type I carcinoma [2, 44, 54]. PTEN inactivation was described in 35% - 50% of all cases of EC type I [66].

In prostate cancers or gliomas PTEN gene alterations were observed in late stages of cancer development [67, 68]. In contrast, in EC, PTEN mutations appear in early stages [44, 69]. Furthermore, the loss of PTEN has been described in histologically normal endometrium before any precancerous lesions could be detected with regular light microscopy [70]. Thus, a causal relation between loss of PTEN function and neoplastic transformation is possible in EC. In normal endometrium, the expression of PTEN protein was shown to correlate with estrogenic stage, being higher during the proliferative phase [71]. AKT phosphorylation can activate ER-α in a "hormone-independent" manner [72]. Other *in vivo* experiments have shown that the loss of PTEN followed by AKT phosphorylation leads to ER-activation independent of estrogenic influence which is usually incriminated in EC type I development [73]. Endometrial glands that lack PTEN undergo abnormal proliferation in an estrogen independent manner [74]. The endometrial glands in normal endometrium do not express high levels of active forms of AKT or ER-α [73]. In vitro studies linked the activation of AKT with the alteration in expression and activity of nuclear ER-α [75]. Pten conditional knockout models had a lower expression of nuclear ER-α in endometrial carcinoma when compared to its precursor, complex atypical hyperplasia [76].

8. Pten Heterozygous Mouse Models

PTEN function is essential for normal development and loss of PTEN plays an important role in carcinogenesis. In order to understand the role of PTEN inactivation in normal development and carcinogenesis, Pten deficient mutant mice have been engineered [9-11, 57]. Homozygous Pten mutant mice proved to be embryonic lethal (from days 6.5 or 7.5 to day 9.5 [9-11], confirming the critical role of PTEN in normal development. Heterozygous mice were compatible with life but developed an array of tumors commonly observed in Cowden's syndrome (associated with PTEN mutations) where there is an increased susceptibility for the development of breast, thyroid, and endometrial cancers [77, 78], demonstrating the function of PTEN as a tumor suppressor gene. The main findings of Pten mutant mice include a wide range of pathological changes such as: colon hyperplasic lesions, hyperplasia of the skin epidermis, prostate, endometrial and thyroid tumors and atrophic changes in seminiferous tubules [9]. Other Pten deficient mouse models presented disruption of the lymphoid lineages with lymph node hyperplasia [10] and myeloid leukemia [11]. The mutants with a different genetic background presented a higher incidence of T cell lymphomas and colon, prostate, endometrium, thyroid and liver tumors [10, 11].

Pten heterozygous (+/-) mouse models demonstrated that female mice develop atypical hyperplasia that progress to carcinoma in endometrial tissue and that biallelic inactivation of Pten occurs early in the progression of the disease [9-11, 57]. Furthermore, potential consequences of biallelic inactivation of Pten were investigated

using a conditional knockout model where Pten was deleted from endometrial tissue using the Cre-Lox system [74, 76]. The conditional Pten deletion in the endometrium had an increased incidence and aggressiveness of the endometrial carcinoma compared to Pten (+/-) mice [76].

9. Pten Deficient Mouse Model and Endometrial Cancer

In our collaborative project with Di Cristofano laboratory, we used a Pten heterozygous mouse model [9] to investigate the 3D nuclear changes of telomeres during endometrial cancer development. The Pten mutations were produced through homologous recombination in mouse embryonic stem cells (ES) (using a 129/SV mouse genetic library). A vector with a functionally inactive Pten allele was used to replace Pten exons 4 and 5. Heterozygous clones (Cj7EC) were injected into C57BL/6 blastocysts and the resulting chimaeric mice were mated with C57BL/6 females to obtain heterozygous Pten (Pten +/-) mice [9].

The endometrial carcinoma (initiation and progression) described in the above mentioned mouse model is very similar to the human EC type I [73]. The development of malignant tumors starts in the endometrial glands with SH followed by AH with cellular atypia and other tissue architectural abnormalities. EC develops from these premalignant lesions in older Pten heterozygous mice.

II. TELOMERES

1. Carcinogenesis

Malignant transformation occurs in normal cells when they escape the normal signaling that controls proliferation and apoptosis [79]. This transformation involves a range of mutations that generate genetic changes leading to tumor development [80]. The normal function of the genome is maintained through DNA repair mechanisms, cell cycle control and apoptosis; when these mechanisms are malfunctioning, the risk for mutations to occur increases, a phenomenon specific to cancer cells [81]. There are two major theories of cancer development: one is the occurrence of successive genomic changes leading to cancer that correlate with progressive tissue alterations [82], the other is the stem cell theory where the genetic alterations (genomic instability) occurs prior to changes detected in cancer, predisposing to subsequent malignant transformation [83].

2. Telomeres Biology and Function

Telomeres are highly specialized structures composed of tandem repeats of 5'-TTAGGG -3' bound to a complex of associated proteins (called the shelterin complex) which cap the single stranded chromosome ends to protect them from abnormal rearrangements [84-86]. The protective function of telomeres against chromosome end-to-end fusions or degradation is due to the loop conformation (T-loop) of telomere ends which masks them so as not to be recognized as DNA breaks [87]. Telomere length is maintained by telomerase, an enzyme reduced in somatic cells [88]. During DNA

replication which occurs in 5’ to 3’ direction, DNA polymerase can add free nucleotides to the 3' end of the new forming strand; consequently, a small portion of the 5’ nucleotide fragment will be lost (end replication problem)[89, 90]. In these cells, telomere DNA is progressively lost with each cell division until the normal cells enter replicative senescence, a protective mechanism to prevent normal somatic cells from genomic alterations to replicate indefinitely [91-93]. In this way, the cells are avoiding abnormal changes and genomic instability due to telomere malfunction. Telomerase is present in stem cells and germ cells which empower them to avoid senescence. Cancer or immortalized cell can acquire the capacity to avoid senescence [94, 95]. Telomere dysfunction may be the cause for telomere shortening or alterations in telomere structure. In cells with the checkpoint defective mechanism, chromosomal instability can be initiated through end-to-end fusion of unprotected chromosomes [96].

The shelterin Protein Complex

Shelterin proteins form a complex structure and play an important role in DNA replication of “fragile” telomeres [97]. This protein complex consists of six proteins: telomeric repeat binding factor 1 (TRF1), TRF2 (telomeric repeat binding factor 2), TRF1 and interacting nuclear protein 2 (TIN2), repressor or activator protein 1 (RAP1), protection of telomeres 1 (POT1) and POT1 and TIN2 interacting protein (TPP1) [98]. By associating with the shelterin complex, telomeres evade DNA damage signaling pathways and double-strand break repair mechanisms at the ends of chromosome, thus solving the end protection problem [99]. Both TRF1 and TRF2 are bound to the double

stranded telomere repeats and are constitutively expressed [100]. POT1 attaches to the single strand DNA overhang [101]. TRF2 was shown to be a “distant homologue” of TRF1 [100]. The balance between TRF1 and TRF2 bound on telomeres is essential for telomere length regulation [102]. Furthermore, TRF2 protects the telomere end by assisting in the stabilization of the telomere loop (t-loop) (t-loop forms as a result of the 3' overhang invading the duplex telomere repeats) [87]. Alterations in t-loop configuration, resulting in 3’-overhang exposure, can leave the telomeres unprotected [87]. As a consequence of these dysfunctional telomeres, cell cycle arrest, cellular senescence or apoptosis may be initiated. Moreover, both TRF2 and POT1 suppress ataxia telangiectasia mutated (ATM) and ataxia telangiectasia and Rad3-related (ATR) signaling pathways, thus, preventing these DNA repair mechanisms from causing end to end fusions of telomeres. These fusions can lead to breakage-bridge-fusion cycles and abnormal chromosome segregation [103, 104]. POT1 also has a role in telomere length maintenance and can reduce the telomere lengthening mediated by telomerase [105, 106]. TPP1 assists POT1 in telomere length maintenance and both regulate telomerase access to DNA [107, 108]. Similar to POT1, TPP1 suppresses the ATR kinase pathway protecting the telomeres against DNA damage response [108]. TPP1 also connects POT1 to TIN2 [109]. TIN2 can bind TRF1 and TRF2 at the same time thus stabilizing the telomere complex [110, 111]. The contribution of RAP1 to shelterin function is less well known. Apparently RAP1 does not bind to the telomere repeats and its recruitment is dependent on TRF2 interaction [112]. Functionally, the shelterin protein complex

protects the integrity of the telomere particularly against chromosomal attrition which is the key to overall genomic stability.

3. Telomeres and Genomic Instability

Genomic instability is defined as an accumulation of genetic alterations which affect the functions of chromosomes and genes [113]. The chromosomes can suffer numerical or structural changes, from simple mutations to aneuploidy (changes of the normal chromosome number). During carcinogenesis, the severity of genetic instability increases and structural changes can coexist with numerical changes [113].

Telomeres play an important role in maintaining genome stability and in controlling cell proliferation [84, 86]. Telomere malfunction can generate both structural and numerical type of genomic instability which can lead to cell immortalization or to transformation to a tumor phenotype [114]. The initial observations were made in 1941 by B. McClintock who described how breakage fusion bridge (BFB) cycles can be initiated in chromosomes and generate anaphase bridges (abnormal chromosomes) [115]. Atypically fused chromosomes will break in the following cell division leading to the random distribution of genetic material [115]. More recently, it was shown that telomeres which lose their protective role due to telomere shortening, telomere aggregation or altered functions of the shelterin complex can generate end to end fusions between chromosomes as a result of activated DNA repair mechanisms [116]. This process continues with abnormal cell divisions and the formation of anaphase

bridges. Further abnormal brakeage leads to increased genomic instability, carcinogenesis and cell death [117].

4. The 3D Organization of the Nucleus

Nuclear architecture and genome organization undergoes dynamic changes correlated with specific functions such as gene expression or DNA replication and repair [118-124]. The genome is highly organized in chromosome territories and chromatin domains [123, 125]. The 3D positioning of chromosomes inside the nucleus dictates genome function [123, 124]. The 3D placement of individual genes has been correlated to their transcriptional activity [126]. Changes of this non random organization can lead to genomic instability and cancer [127-129].

5. The 3D Organization of Telomeres inside the Nucleus

The analysis of the 3D nuclear architecture of telomeres in interphase nuclei is a relatively new technique in the study of genomic stability in normal and cancer cells [127, 129, 130]. Fluorescence microscopy combined with quantitative image analysis enables us to characterize the 3D organization of telomeres inside the nucleus [127]. The 3D telomere organization in the nucleus is cell-cycle dependent and telomeres form a disk in G2 [131]. Also, telomeres are engaged in a dynamic process that shows cell-type specificity [127]. Comparison between normal and neoplastic lymphocytes showed changes in the 3D architecture of telomeres in cancer cells with the telomeres assembling into aggregates in neoplastic lymphocytes [132]. Following the formation of

telomeric aggregates, chromosomes can fuse and form anaphase bridges that can break and generate unbalanced translocations and terminal deletions causing the genomic instability characteristic of cancer cells [132].

6. Microscopy and Imaging

Modern light microscopy started when Köhler illumination was first introduced in 1893 by August Köhler, who developed for the first time a special method of specimen illumination for both transmitted and reflected light [133]. Methods of illumination in microscopy were improved further by F. Zernike [134] who developed phase contrast illumination and G. Nomarski [135] who discovered differential interference contrast microscopy. During the later decades, the main challenge in microscopy was to overcome the limits in resolution.

7. Fluorescent Microscopy

Fluorescence is defined as the emission of light from a substance generated after the absorption of excitation light with a shorter wavelength. The first observations were made by the British scientist George Stokes in the nineteenth century. He observed that the emitting fluorescent light has a longer wavelength than the excitation light and today this difference is called “Stokes shift”. The fluorescent molecules are seen because the excitation light can be filtered and just the fluorescent emission can pass through (using dichroic mirrors). Molecules with fluorescent properties are called fluorophores. Some of the main characteristics of fluorophores are the specific affinity for the target (chemical attraction and complementarity) and the emission efficiency

(named quantum yield); because of these characteristics, their biological use is very successful. Fluorescent microscopy permits 3D visualization by collecting images with high resolution at the subcellular level [136-139]. The disadvantage of imaging using wide-field microscopy is that images collected in the axial plane are blurred due to the out of focus light [139, 140].

8. Resolution of Light Microscopy

Resolution is the ability to distinguish two objects as being separate. In order to see subcellular structures, objects inside a cell must be resolved from one another. Conventional microscopy has a resolution limit, described for the first time in 1873 by Abbe [141] , caused by one of the properties of light, diffraction. Light coming through the lens aperture forms a diffraction pattern known as an airy pattern; the spatial representation of the diffraction pattern is called the point spread function (PSF) [142]. The limit of resolution can be quantified in both lateral and axial planes using a special criterion named Rayleigh criterion: d (lateral) =0.61 λ/ NA and d (axial) = 2 λ / NA^2 (λ=wavelength of light, NA=numerical aperture). The conventional limit of resolution was overcome in the last decades [138] by new methods as: 4pi-microscopy [143] , localized microscopy [144] and structured illumination [145].

In our study we used a combination of wide field optical sectioning and image deconvolution combined with volume rendering to create a 3D view. The first Charge Coupled Devices (CCDs) were invented in 1969 by George Smith and Willard Boyle [146] . This device captures images similar to an electronic film and converts an optical image

into an electronic signal [147]. Its function is to integrate the image on a chip. The main characteristics of this device are: high resolution, high sensitivity and a wide dynamic range [147, 148].

9. Deconvolution

Deconvolution was described for the first time by Agard and Sedat in 1983 [139]. They demonstrated that resolution can be improved in 3D microscopy by processing the images using specific algorithms [139]. Deconvolution involves a computerized image processing of the quantitative information acquired by axial section imaging [137]. The out-of-focus light is reassigned to its initial location and thus the deconvolution algorithms improve resolution [136, 139]. In 3D quantitative fluorescence microscopy, non-iterative [149], constrained iterative [139, 150, 151] or blind [152] deconvolution algorithms are most common.

In our investigation we used constrained iterative deconvolution [151].

10. Fluorescence in Situ Hybridization

Fluorescence in situ hybridization (FISH) is a cytogenetic method used for the detection of DNA and RNA sequences in different types of cells and tissues [153]. Using this technique, we can locate specific DNA sequences of interphase chromatin or metaphase chromosomes using fluorescent probes that bind to the corresponding DNA sequences. Based on this principle, FISH is a very sensitive method used to identify structural and numerical chromosomal changes [153]. The first use of fluorescence in

situ hybridization was in 1980 when an RNA sequence was labeled with a flourochrome molecule at the 3' end and used as a probe for targeting DNA sequences [154]. Interphase FISH is one of the specific methods used to investigate chromosomal aberrations using the interphase nuclei as targets for hybridization; a large number of cells can be screened and the resulting data can be statistically analyzed [155].

In recent years, more and more studies have used FISH to study nuclear architecture. FISH combined with 3D image analysis was used to investigate the dynamics of replication sites inside the "individual chromosome territories" [156]. Furthermore, the organization of higher order chromatin proved to be preserved during the 3D FISH procedure "down to the level of approximately 1-Mb chromatin domain positions" [157]. For this study, a CY3-labelled PNA telomere probe $(CCCTAA)_n$ was used to specifically hybridize and visualize repetitive telomeric DNA sequences.

Chapter II: MATERIAL AND METHODS

A total of 59 paraffin embedded uterine tissue samples were collected for this project. Of these, 28 samples were collected from WT mice and 31 samples were collected from Pten heterozygous mice. All mice had the same genetic background. The age of the mice ranged from 3 to 22 months (table 1).

1. Tissue Sectioning and H&E Staining

Paraformaldehyde fixed and paraffin embedded uterine tissues were sectioned at 5µm. Haematoxylin and eosin (H&E) staining was performed for morphological analysis.

Tissue slides were deparaffinized in 2 changes of xylene, 15 minutes each, and rehydrated in 2 changes of 100% alcohol, 5 minutes each, followed by 95% alcohol for 2 minutes and 70% alcohol for 2 minutes. After a brief wash in distilled water, sections were stained with Meyer's haematoxylin for 8 minutes, washed in running tap water for 5 minutes and differentiated in 1% acid alcohol for 30 seconds. Next, the slides were washed in running tap water for 5 minutes and placed in saturated lithium carbonate solution for 2 minutes followed by washing in running tap water for another 5 minutes. After being rinsed in 95% alcohol for 1 minute, slides were counterstained in eosin-phloxine B solution for 2 minutes, dehydrated in 95% alcohol for 1 minute and 2 changes of absolute alcohol for 5 minutes each. Before mounting with xylene based mounting medium, the slides were cleared in 2 changes of xylene for 5 minutes each.

2. Immunohistochemistry: PTEN

PTEN expression was detected by immunohistochemistry. Paraffin embedded blocks of endometrial tissue of wild type and Pten heterozygous mice were cut at 5 µm and dried overnight at 37 °C. Next, slides were kept at 60 °C overnight to soften the paraffin, followed by dewaxing in xylene two times, 10 minutes each at RT and rehydration in descending alcohol baths: 100%, 90%, 70%, 60% and 50% ethanol for 3 minutes each. Slides were washed with double distilled water and then equilibrated in TBS (pH=7.4) buffer for 10 minutes at room temperature. After blocking the endogenous peroxidase in 3% hydrogen peroxide in methanol, slides were washed in TBS (pH=7.4) buffer two times, 10 minutes each. Slides were incubated in 10mM citrate buffer (pH 6.0) for 30 minutes at 90 °C for antigen retrieval. After cooling for 20 minutes at room temperature, two washes in TBS (pH=7.4) buffer, 10 minutes each, was done. Tissue sections were blocked with 10% NGS (normal goat serum) in TBST and incubated overnight at 4°C with the primary antibody (PTEN polyclonal, Abcam) using a 1:100 antibody dilution in the same blocking buffer. On the second day, slides were washed in TBS (pH=7.4) buffer two times, 10 minutes each, to remove the primary antibody, and then incubated with biotinylated secondary antibody (goat anti-rabbit), 1:200 in TBS buffer for 1 hour at room temperature. After three 5 min washes, ABC (Vectastain ABC kit, #PK-6105) was applied for 30 minutes at room temperature. Three 5 min washes were performed before visualize the reaction using the HRP-substrate DAB (DAB #34002, Thermo Scientific) by developing the slides for 10 minutes. Sections were counterstained with Harris"s haematoxylin, dehydrated in

ethanol and coversliped with xylene-based Permount™ for imaging. Rabbit polyclonal IgG (Abcam) was used as a negative control.

Images were taken with the Axio Imager A1 microscope coupled to an AxioCam ICc3 camera and the AxioVision software version 4.8 (Carl Zeiss, Canada).

3. Telomere Fluorescence in-Situ Hybridization (FISH)

Mouse wild type (wt) and Pten heterozygous slides were deparaffinized three times for 10 minutes each and further dehydrated two times, one minute each, in 100% ethanol. Slides were incubated in 1 M NaSCN (sodium thiocyanate) for 30 minutes at 80 °C in a water bath to unmask target DNA sequences in the dewaxed tissue slides. After a 3 minutes rinse in double distilled water, slides were incubated in 3.7% buffered formalin solution (Sigma-Aldrich) in 2x SSC buffer (pH 7.6) for 10 minutes at room temperature and washed two times in 2xSSC for 5 minutes each. 50 µg/ml pepsin was added to 0.01 M 37 °C prewarmed hydrochloric acid (HCL) and slides were incubated for 6 minutes followed by two washes in 2xSSC for 5 minutes each. After reincubating the slides in 3.7% buffered formalin solution (Sigma-Aldrich) in 2x SSC buffer (pH 7.6) for 10 minutes at room temperature and washed two times in 2xSSC for 5 minutes each, we dehydrated tissues in 70%, 90% and 100% ethanol for 1 minute each.

5 µl of Cy3-labeled peptide nucleic acid telomere (PNA) probe (Dako, Denmark) was applied to each slide to detect $(T2AG3)_n$ repeats . Slides and probe were incubated at 80°C for 3 minutes to denature DNA, followed by hybridization at 30°C for 2 hours using Hybrite (Vysis, Abbott Diagnostics). Next, slides were washed twice for 15 minutes in

70% formamide in 10 mM Tris (pH 7.4) followed by successive washings: in 1× PBS at room temperature for 1 minute, in 0.1× SSC at 55°C for 5 minutes and in 2× SSC in 0.05% Tween 20 twice for 5 minutes each. Slides were counterstained with 4′,6-diamino-2-phenylindole (DAPI) (0.1 µl/ml), washed in doubled distilled water and dehydrated in 70%, 90%, and 100% ethanol, 2 minutes each. Before imaging, slides were mounted to coverslips using Vestashield antifade mounting medium (Vector Laboratories, Canada).

Buffer Composition

20X SSC: 175.3 g of NaCl and 88.2g of sodium citrate were dissolved in 800 ml of distilled water. pH was adjusted to 7.0 with a few drops of 1M HCl. The total volume was adjusted to 1 L with additional distilled water.

Tris-Buffered Saline (TBS): 8 g of NaCl and 3 g of Tris base were dissolved in 800 ml of distilled water. The pH was adjusted to 7.4 with a few drops of 1M HCl. The total volume was adjusted to 1 L with additional distilled water.

Citrate buffer: stock solution A (21,01 g citric acid in 1000 ml distilled water) and stock solution B: 29,41 g sodium citrate in 1000 ml distilled water.

4. Image Acquisition

Fluorescent images were captured using a AxioImager Z1 microscope, an AxioCamMR3 camera and a Plan-Apochromat 63x/1.40 Oil DIC M27 lens (all from Carl Zeiss, Canada). Acquisition time was 300 milliseconds for Cy3 (telomeres signals) and

100 milliseconds for DAPI (nuclear DNA stain). For each image, 60 vertical stacks (z-stacks) were acquired with a sampling distance of the x and y axis of 107 nm and z axis of 200 nm using AxioVision 4.8 software (Carl Zeiss, Canada).

5. Image Analysis

For each histological type of glandular epithelium (normal, simple hyperplasia, atypical hyperplasia, and carcinoma) of individual slides, 30 nuclei were selected for analysis. Individual images of each nucleus from the acquired images were produced for further analysis. Constrained iterative deconvolution [151](a mathematical algorithm that restores the image clarity in 3D) of each individual nucleus was achieved by using the AxioVision 4.8 software (Carl Zeiss, Canada). Next, the deconvolved images were converted to TIF files for three-dimensional analysis using the TeloView software.

TeloView is a software tool that was developed to detect probe signals inside the 3D nucleus and to quantify signal intensities [131]. TeloView calculates the intensities of the telomere signal in the 3D image and defines the positions where telomeres are distributed in the nucleus.

By using statistical analyses, telomere aggregates are calculated for each image using a predefined threshold. The TeloView software was originally developed to render the number of aggregates formed by human telomeres but the signal threshold for aggregates in normal mouse nuclei has been calculated in Dr. Mai's laboratory more recently. Thus, both mouse and human telomere aggregates can be assessed.

6. Statistical Analysis

As a result, Teloview can be used to determine the following: (1) the number of telomeric signals per nucleus, (2) the 3D distribution of telomere signals inside the nuclear volume, (3) the number of telomere aggregates calculated per nucleus, and (4) the distribution of the intensity of the florescent signal emitted by the telomere probe.

For each comparison of telomere signals, distribution of the Frequency table and Chi-square test procedure was used to test the correlation between two parameters: the number of telomere signals and signal intensity. Analyses were performed using SAS v9.1 software.

Chapter III: RESULTS

1. Endometrial Pathology

Sample characteristics are summarized in Table 1.

We did not detect any endometrial pathology in uterine sections from 28 WT mice. In contrast, examination of H&E staining of uterine tissue sections from 31 Pten heterozygous mice revealed endometrial pathology such as: SH, AH and EC. We noticed progressive alteration of endometrial glandular architecture during different age points. In some animals, we observed a complex pathological appearance where different pathologies such as SH and AH or AH and EC coexisted in the same endometrial tissue. In some tissues, EC was already developed in 5 month old mice. We observed the first pathological changes in the endometrial glands in very young Pten heterozygous mice (3 months). These changes were apparent in epithelial compartment, with hyperplasia of endometrial glands and an increase in glandular density in relation to stroma reflecting the increase in glandular cross sections. The glands appeared crowded but distinctly separated by a wide stromal layer. The diameters of the glands in SH samples were similar to those observed in the normal endometrial tissue of the WT control mice. This crowded SH glandular pattern (Fig.1) coexisted with a normal glandular distribution in non-affected areas. The endometrial glands became more irregular in size and shape and more crowded in older Pten heterozygous mice (3-7 months). AH was characterized by a stratification of the glandular epithelial cells with loss of cell polarity (loss of cell orientation in relation to the basement membrane) and atypical nuclei (enlarged nuclei

of various sizes with vacuolar appearance of the chromatin and prominent nucleoli) (Fig.2). The glands in AH appeared more crowded than glands in SH but they were still separated by a thin stromal layer and a visible basal membrane. In some animals, different areas of endometrial tissue had different coexisting pathologies such as SH and AH.

Malignant transformation of the glandular epithelium occurred between 5 and 12 months (Fig. 2). A number of Pten heterozygous animals had both AH and EC pathologies. In EC, the glandular architecture was completely lost, with confluent enlarged glands that were not separated by stroma, with atypical nuclei, necrotic cells and loss of cell polarity. Some EC samples showed cystic enlargement with a huge lumen filled with debris and necrotic cells. Some EC did not have any lumen but appeared as a solid carcinoma cell mass. This tumor pattern of the epithelial compartment involved very large portions of the endometrial tissue. Stromal tissue changed to an altered fibroblastic appearance infiltrated by malignant cells of various sizes. We observed glands with a cribriform aspect (pseudoglandular) consisting of distinct areas of back-to-back positioned glandular structures where the cells formed curved structures with no intervening stroma and where the basal membrane was no longer identified. In some advanced EC sample, malignant cells invaded the muscle layer of the endometrium.

Table 1 Endometrial Mouse Tissue Sections

We analyzed the endometrial tissue material from a total number of 59 animals. A number of 28 animals were WT (wild type) and 31 animals were Pten (+/-) heterozygous animals. The endometrial pathology observed in the mutant mice was classified in SH (simple hyperplasia), AH (atypical hyperplasia) and EC (endometrial carcinoma).

Slide	Age		Pathology				Slide	Age		Pathology		
		WT	**SH**	**AH**	**EC**				**WT**	**SH**	**AH**	**EC**
M1	3 mo		x	x			M31	9mo	x			
M2	3 mo		x	x			M32	9mo	x			
M3	3 mo		x	x			M33	9mo	x			
M4	3mo	x					M34	9mo	x			
M5	3mo	x					M35	10 mo			x	x
M6	5 mo		x	x			M36	10 mo				x
M7	5 mo		x	x			M37	10 mo				x
M8	5mo	x					M38	10 mo				
M9	5mo	x					M39	10 mo			x	
M10	5mo	x					M40	11 mo				x
M11	5mo	x					M41	11 mo			x	x
M12	5mo	x					M42	11 mo				x
M13	6 mo			x	x		M43	11 mo			x	x
M14	6 mo			x	x		M44	11 mo			x	x
M15	6 mo		x	x			M45	11 mo			x	x
M16	6 mo		x	x			M46	11 mo			x	x
M17	6 mo		x	x			M47	11mo	x			
M18	6mo	x					M48	11mo	x			
M19	6mo	x					M49	11mo	x			
M20	7 mo				x		M50	11mo	x			
M21	7 mo			x			M51	11mo	x			
M22	7 mo			x			M52	11mo	x			
M23	7mo	x					M53	12 mo				x
M24	8 mo				x		M54	12 mo			x	x
M25	8 mo				x		M55	12mo	x			
M26	8 mo			x			M56	12mo	x			
M27	8mo	x					M57	12mo	x			
M28	9mo	x					M58	13 mo			x	x
M29	9mo	x					M59	22mo	x			
M30	9mo	x					**No**		**28**	**8**	**22**	**18**

<u>Fig. 1</u> Normal Endometrial Glands in WT Mice and Simple Hyperplasia in Pten Mutant Mice

Representative H&E staining of uterine sections of a WT and Pten heterozygous mouse (both 3 months old) showing normal glandular morphology (WT) and simple hyperplasia lesions (SH) with increased gland/stroma ratio (increased number of crowded glands).

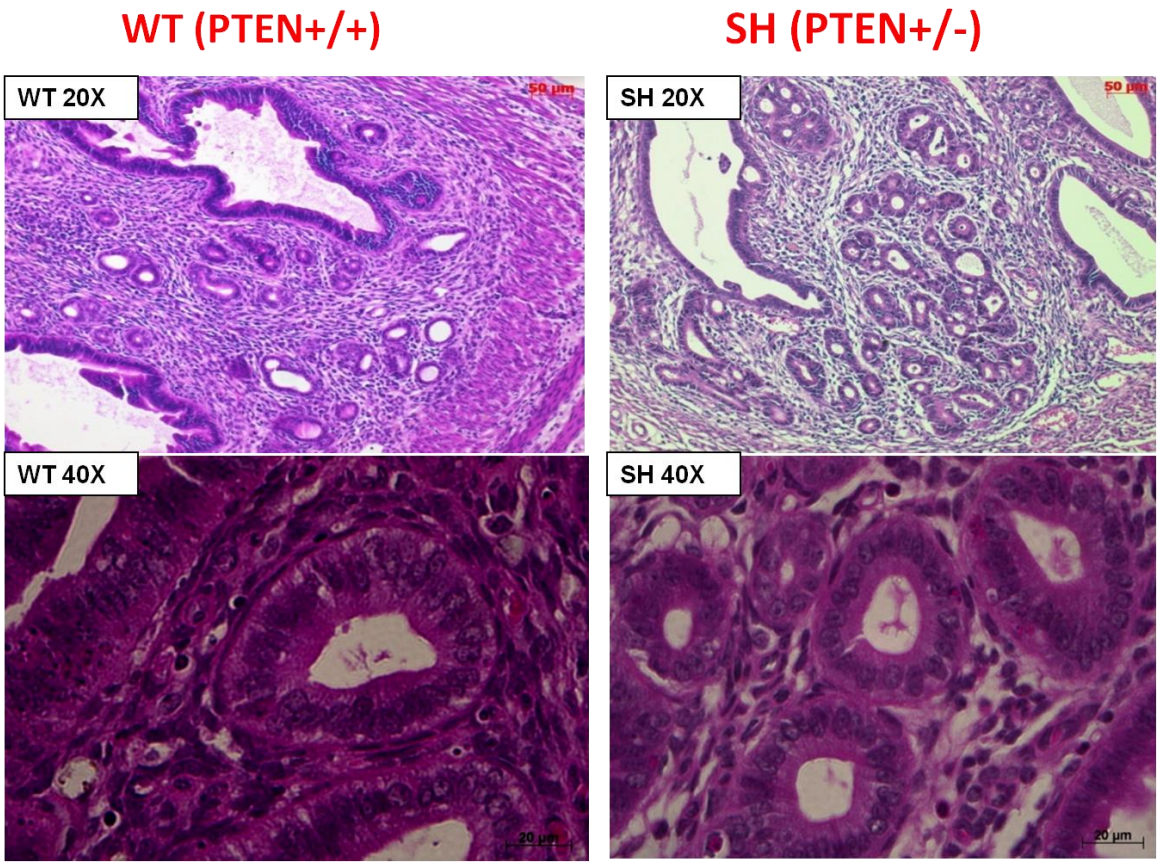

Fig. 2 Atypical Hyperplasia and Endometrial Carcinoma in Pten Mutant Mice

Representative H&E staining of uterine section of Pten heterozygous mouse (6 months) showing lesions characteristic of atypical hyperplasia (AH) with stratified glandular epithelium, crowded glands of various sizes separated by a thin layer of stroma and an increased gland/stroma ratio. Some glandular cells did not arrange towards the basal membrane (loss of polarity). Nuclear atypia with enlarged nuclei, vacuolar appearance and prominent nucleoli can be observed; Pten heterozygous mouse (12 months) showing endometrial carcinoma (EC) lesions with multi-layered epithelium, atypical nuclei, altered fibroblastic stroma and invading cancer cells. The back to back glands appeared fused, with no intervening stroma and no basal membrane present (cribriform aspect).

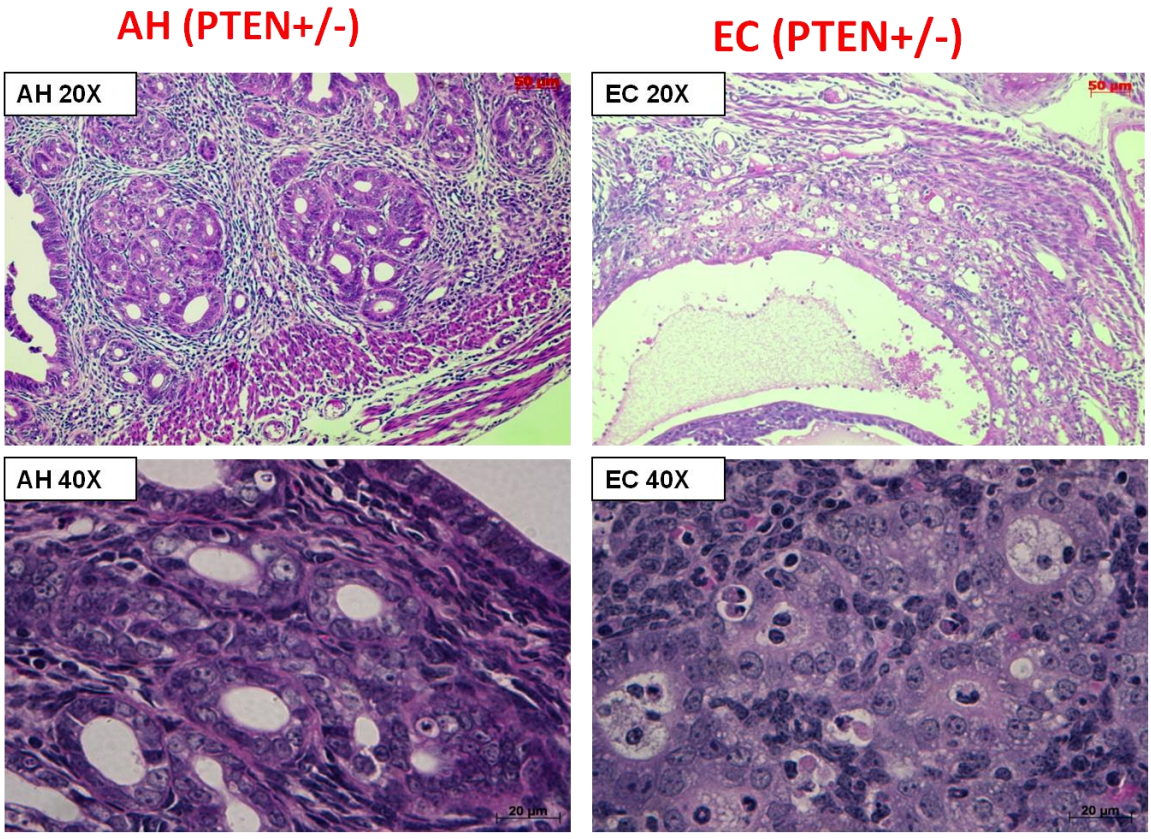

2. PTEN Immunoreactivity

PTEN immunoreactivity was tested on uterine serial sections of wild-type (WT) and Pten heterozygous mice (Figs.3, 4). Immunostaining with the PTEN antibody on uterine sections of mice presenting different pathologies revealed different outcomes. PTEN loss was an early event in endometrial carcinoma development. In WT mice, the endometrial glands have a nuclear expression of PTEN that shifts towards a more cytoplasmic expression once SH pathology occurs in the tissue of Pten heterozygous mice. In AH and EC pathology, PTEN protein expression decreases significantly until it was completely lost. Endometrial PTEN was expressed in both the nucleus and cytoplasm of SH glands of Pten heterozygous mice. Compared to endometrial glands of WT mice that express the PTEN staining mainly in the nucleus, SH glands of Pten heterozygous mice express PTEN predominantly in the cytoplasm. Stromal and epithelial cells were also PTEN positive in both WT and SH mouse endometrium (Fig. 3). Older Pten heterozygous mice that developed AH showed a decreased expression of PTEN with exclusively cytoplasmic localization or a complete loss of PTEN immunoreactivity. No nuclear PTEN expression was detected (Fig. 4). Loss of PTEN immunoreactivity, possibly due to the inactivation of the remaining allele, was observed in EC tissue (6 to 13 months old mice). Most of these sections showed signs of carcinoma cell invasion (Fig. 4).

<u>Fig.3</u> PTEN Expression in WT and SH Endometrial Tissue

PTEN immunostaining of uterine sections of normal endometrium (WT mouse) and simple hyperplasia (Pten mutant mouse). Normal endometrial glands show PTEN nuclear (arrow) and cytoplasmic immunostaining. The Pten heterozygous mouse shows SH with mainly cytoplasmic and some nuclear (arrow) PTEN localization in the endometrial glands (3 months). Negative control (insert).

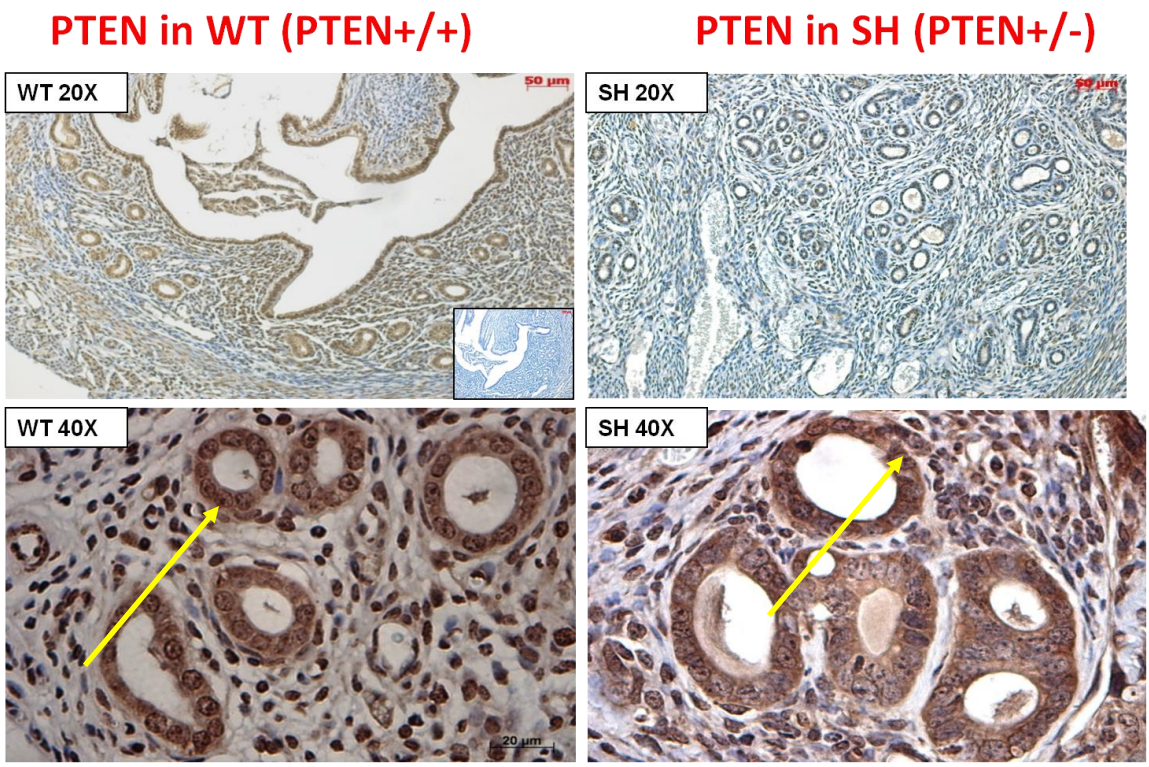

Fig.4 PTEN Expression in AH and EC Endometrial Tissue

PTEN immunostaining of uterine sections of Pten heterozygous mouse (6 months) showing AH with reduced immunostaining for PTEN and lack of nuclear PTEN and Pten heterozygous mouse (12 months) showing EC with loss of PTEN protein expression in carcinoma lesions.

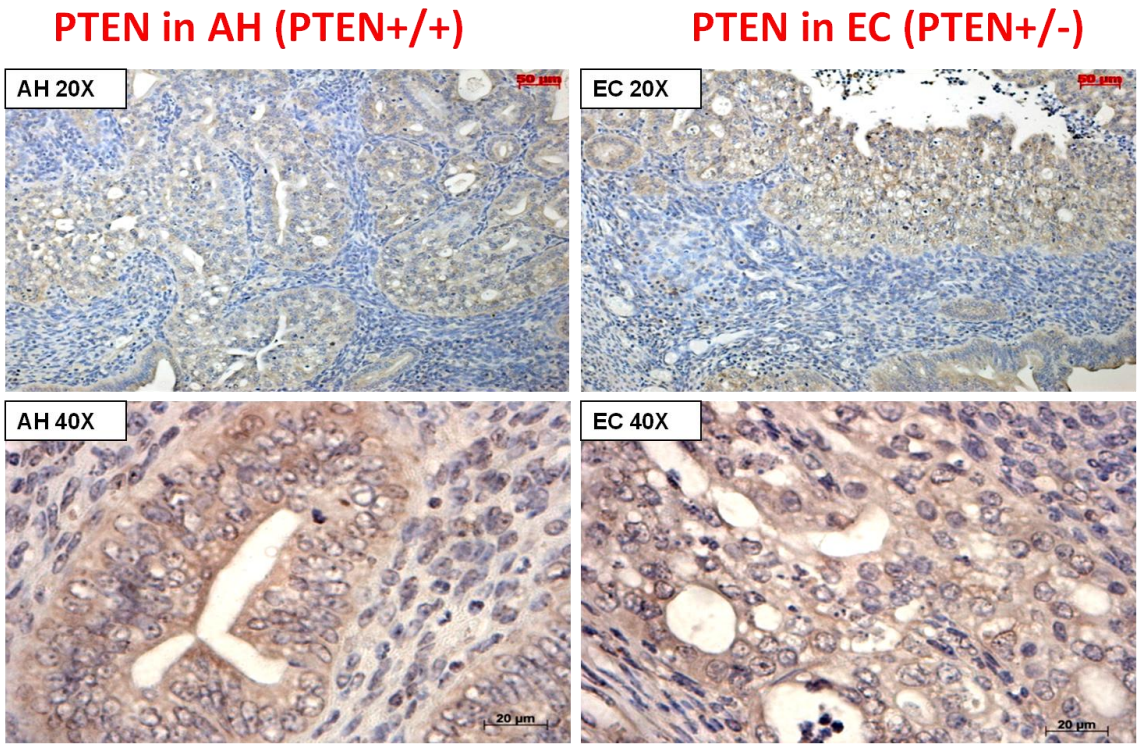

In summary, we have shown that immunoreactive PTEN was localized in the nucleus and the cytoplasm in WT glandular epithelial cells. In Pten heterozygous mice, we observed a shift towards cytoplasmic localization in SH, and the cytoplasmic expression of PTEN was gradually lost during AH to EC progression.

3. FISH and Imaging

5 µm serial uterine sections from WT and Pten heterozygous mice were used for the investigation of the 3D telomere nuclear architecture. Fig. 5 illustrates the fluorescence in situ hybridization (FISH) of normal endometrial glands, where nuclei (blue DAPI staining) and telomere signals (red Cy-3 staining) are identified.

Based on different histological appearances, individual nuclei where marked, coded and selected for image processing and analysis. In our current study, we analyzed only the glandular epithelial cells of WT and Pten heterozygous mice. Consequently, for mutant mice, we selected glandular cells where SH, AH or EC pathologies were observed. Based on the DAPI images of the nuclei in conjunction with the corresponding H&E serial sections, we selected the nuclei of glands presenting clear characteristics of a particular pathology. Nuclei that overlapped other nuclei or that lacked nuclear integrity were excluded from further analysis. We did not consider other criteria for rejecting a cell for analysis. Telomere nuclear signals of specific Pten heterozygous mice uterine pathology (SH, AH and EC) in 2D and 3D (after reconstruction using deconvolution) are illustrated in Figs. 6 and 7.

Fig. 5 FISH Image of Normal Endometrial Glands

(a) FISH image of normal endometrial glands (ZEISS, Axio Imager Z1 Plan-Apochromat 63x/1.40 Oil DIC M27AxioCamMR3). Shown here is an example of an individual nucleus: (b) DAPI image, (c) Cy3 detection (d) Fluorescent composite image (DAPI +Cy3). The images (b) to (d) show a representative sectional fluorescence image of the 60 image sections taken of this individual nucleus.

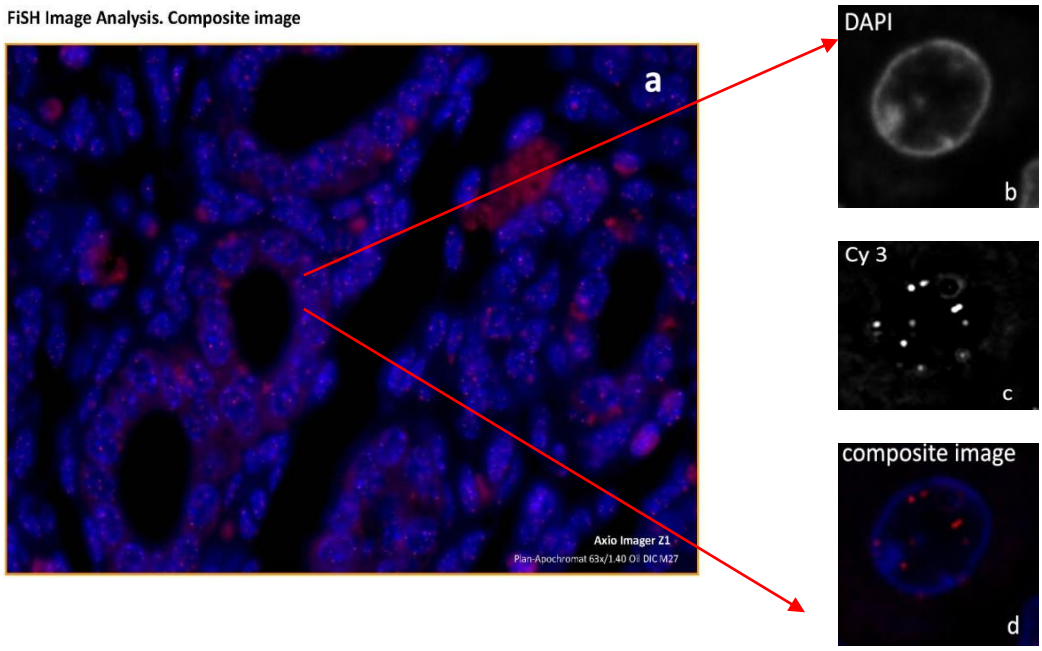

Fig. 6 DAPI Fluorescence Images after Telomere FISH

(A-C) DAPI fluorescence images after telomere FISH. The figure is showing the numbered nuclei analyzed with TeloView. Example of a single nucleus (D-F) within a gland showing SH (A), AH (B), and EC (C). 2D visualization of the telomere hybridization signals within the single nucleus (D-F)

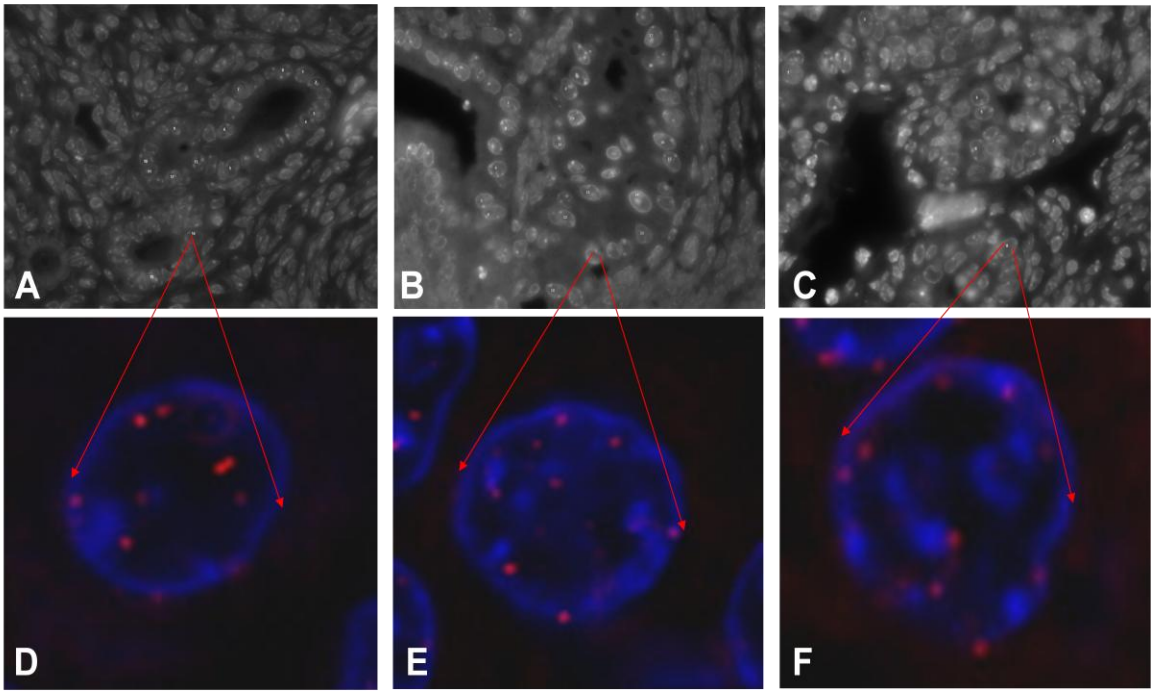

Fig. 7 3D Reconstruction of the Telomere Hybridization Signals

The figure is showing representative examples of telomere signals within a single nucleus of a glandular cell from (A) SH, (B) AH and (C) EC endometrial tissue (Pten heterozygous mice). Arrows indicate the formation of telomere aggregates (fused telomeres).

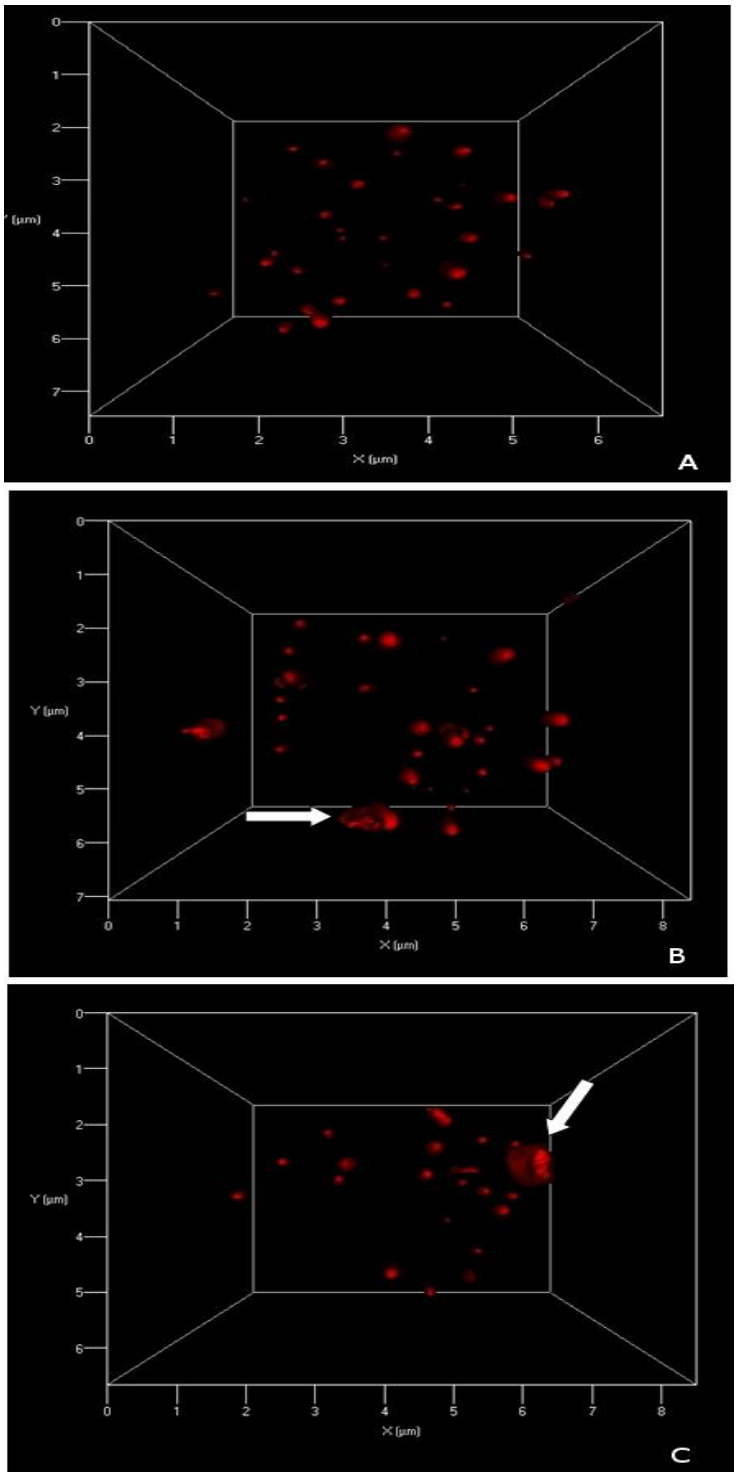

Fig. 8 Teloview Software [131]

This software measures telomere intensity signals and 3D telomere position inside the nucleus.

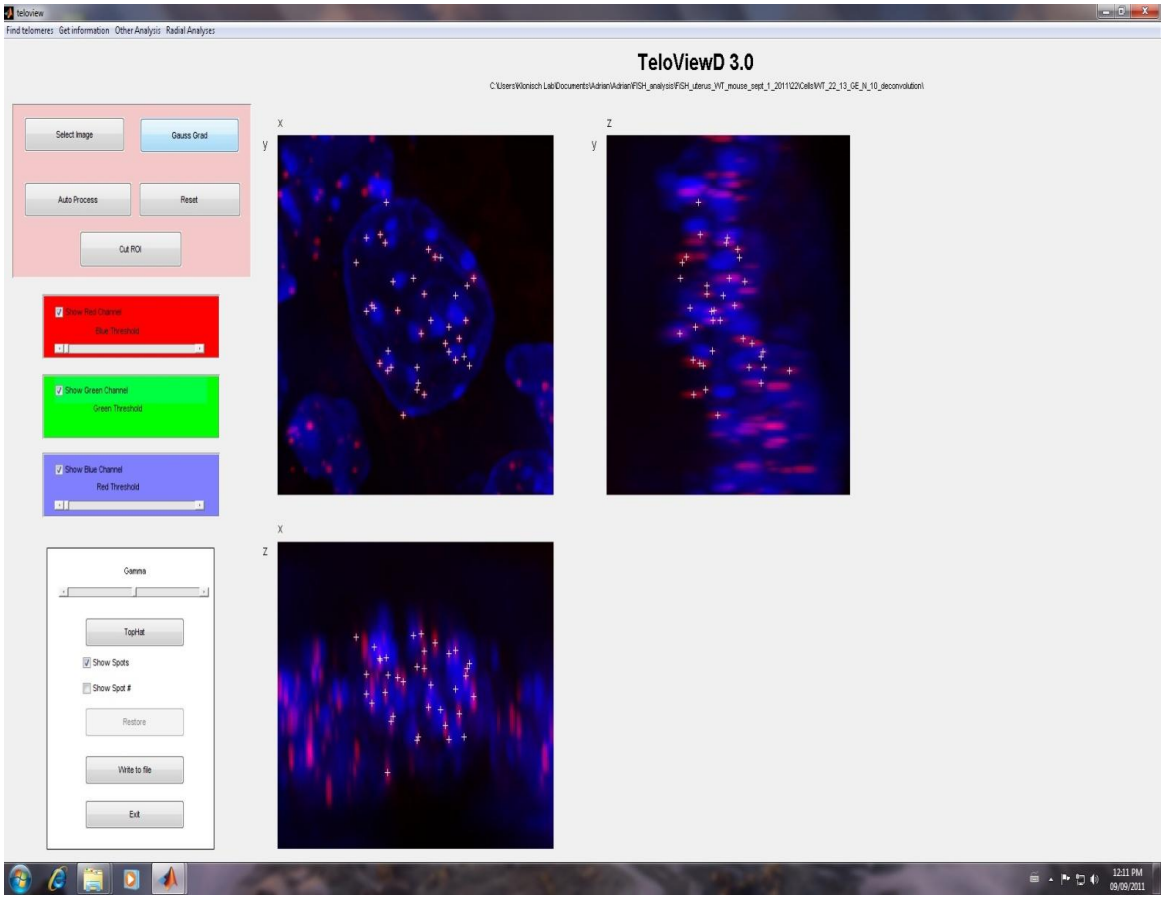

4. Telomere Length and Telomere Signals Distribution

The relative intensity of telomere signals is correlated with telomere length [158]. The number of telomeres showing a specific intensity of fluorescent signal was quantified using the Teloview software (Fig. 8). Low intensity signals corresponded to shorter telomeres and the high intensity signals corresponded to longer telomeres. 30 nuclei were analyzed for each animal and histological category. For individual animals showing two histological categories, 30 nuclei from each category were analyzed. The histograms (Figs. 9-12) provide representative examples for the telomere profile for each histology group (in one animal) of 30 cells. We analyzed a total number of 28 samples from WT mice and 48 samples from Pten heterozygous mice: 8 samples with SH pathology, 22 samples with AH pathology and 18 samples with EC pathology. Statistical data from all these categories is summarized in Fig.13. According to the telomere profile determined, four intensity groups were used for statistical analysis: <6,000; 6,000-10,000; 10,000-20000; >20,000 (Fig. 13). We did not detect any significant changes in telomere length among different ages in wild type mice and consequently we did not consider age as a factor for our analysis, but we analyzed different histopathologies.

SH had a significantly higher number of telomeres in the <6,000 group and a significantly lower number of telomeres in the 10,000-20,000 group compared to WT. There were no significant differences in the telomere intensity distribution of AH and EC compared to WT, except in 6,000-10,000 group where AH had a significantly lower number of short telomeres compared to WT.

To better characterize the telomere signal distribution in cells of the same endometrial tissue expressing the same pathology, we grouped the signals into different bins (Figs. 9-12). The cells of Pten heterozygous mice more often showed a heterogeneous population of cells when compared to cells in control mice. We found this pattern in all pathological categories including simple hyperplasia, atypical hyperplasia and carcinoma.

<u>Fig.9</u> Telomere Distribution in WT

Example of telomere intensity distribution in the endometrial glandular cells of WT mice. A total of 30 nuclei were analyzed. This figure illustrates the number of telomere signals (y axis) having a specific telomere intensity (x axis) corresponding to telomere length.

Insert: The number of telomere signals in WT mouse endometrial glandular cells grouped in different bins. The figure illustrates the distribution of the number of nuclei (y axis) having a specific number of telomere signals (x axis). The total number of nuclei is 30. The single-curve pattern was the most frequently encountered in our controls, indicating a homogenous population of cells regarding the number of signals per nuclei.

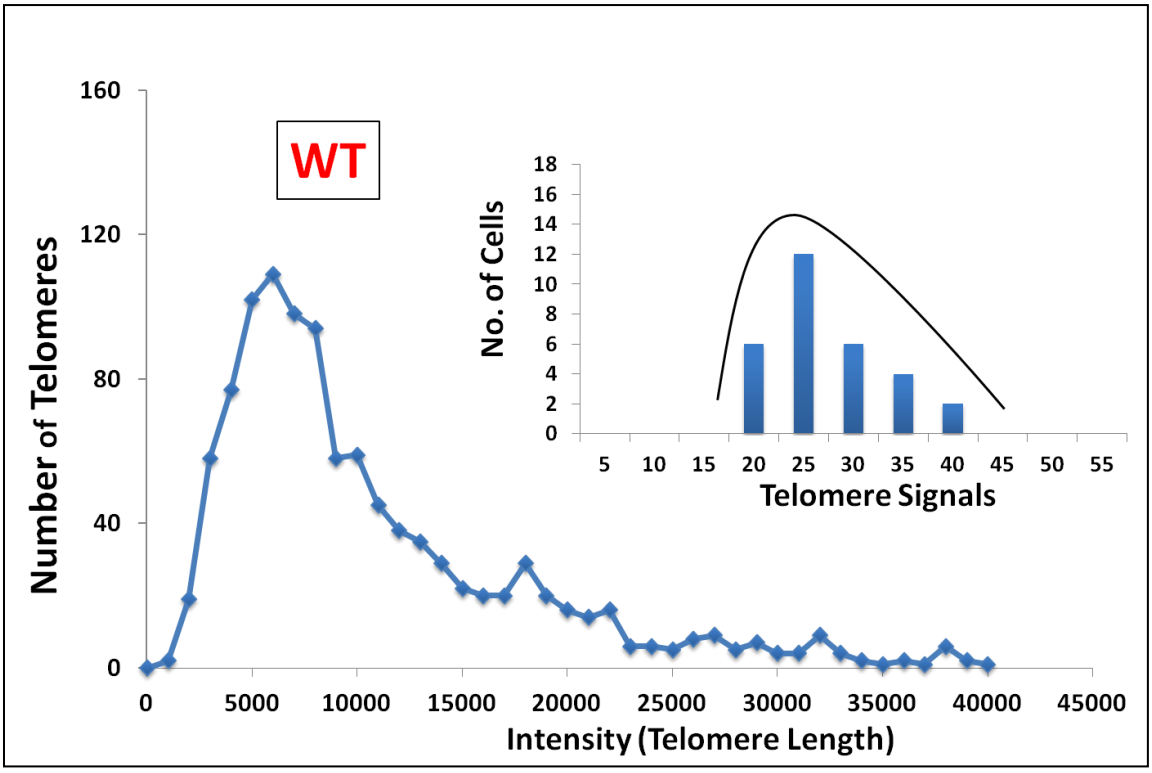

<u>Fig.10</u> Telomere Distribution in SH

Example of telomere intensity distribution in the endometrial glandular cells with SH in Pten heterozygous mice. This figure illustrates the number of telomere signals (y axis) having a specific telomere intensity (x axis) corresponding to telomere length. A total of 30 nuclei were analyzed. A significantly higher number of short telomeres was found in SH pathology compared to WT.

Insert: The number of telomere signals in Pten heterozygous mouse endometrial glandular cells grouped in different bins (SH pathology). The figure illustrates the number of nuclei (y axis) having a specific number of telomere signals (x axis). A two-curve pattern was frequently encountered in SH, indicating a heterogeneous population of cells regarding the number of signals per nucleus.

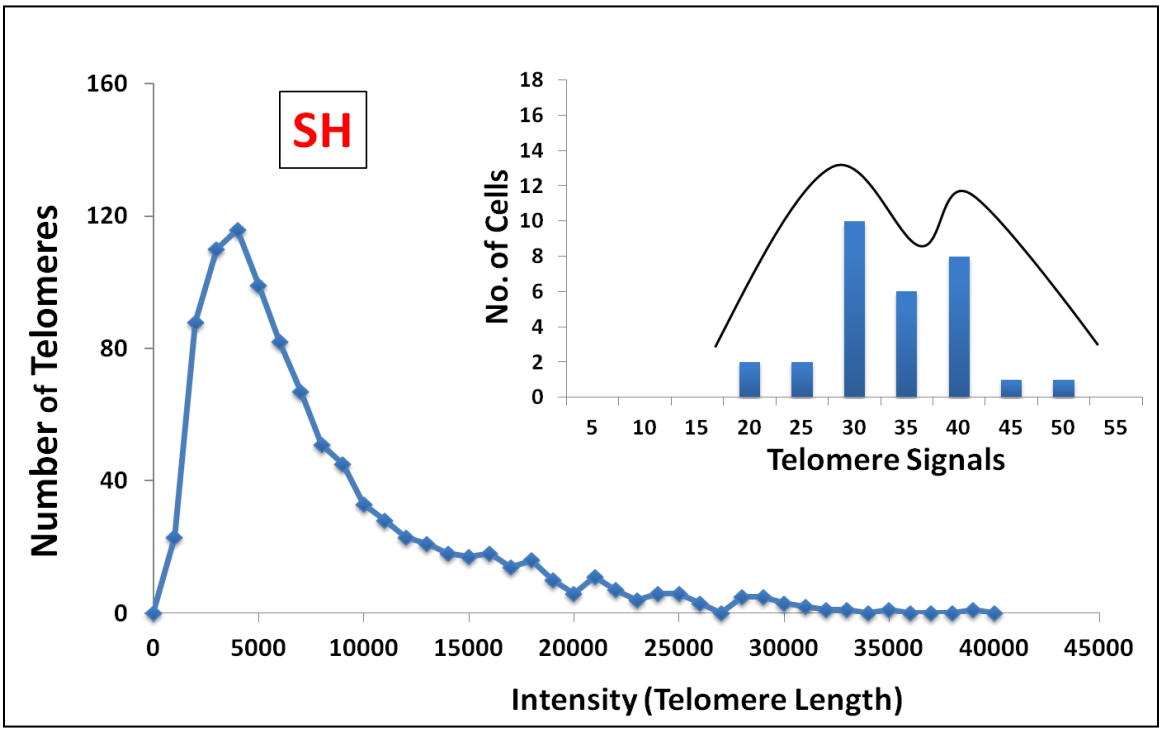

Fig.11 Telomere Distribution in AH

Example of telomere intensity distribution in the endometrial glandular cells with AH in Pten heterozygous mice. This figure illustrates the number of telomere signals (y axis) having a specific telomere intensity (x axis) corresponding to telomere length. A total of 30 nuclei were analyzed.

Insert: The number of telomere signals in Pten heterozygous mouse endometrial glandular cells grouped in different bins (AH pathology). The figure illustrates the number of nuclei (y axis) having a specific number of telomere signals (x axis). The two-curve pattern was also frequently encountered in AH, indicating a heterogeneous population of cells regarding the number of signals per nucleus.

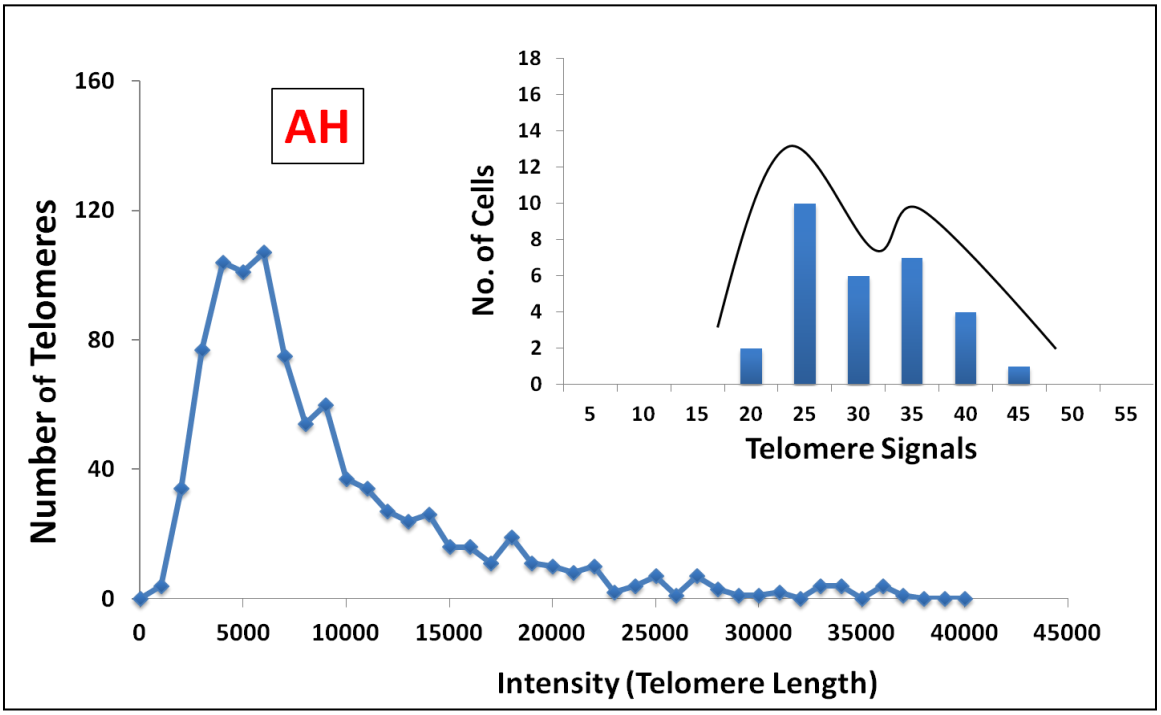

Fig.12 Telomere Distribution in EC

Example of telomere intensity distribution in the endometrial glandular cells with EC in Pten heterozygous mice. This figure illustrates the number of telomere signals (y axis) having a specific telomere intensity (x axis) corresponding to telomere. A total of 30 nuclei were analyzed.

Insert: The number of telomere signals in Pten heterozygous mouse endometrial glandular cells grouped in different bins (EC pathology). The figure illustrates the number of nuclei (y axis) having a specific number of telomere signals (x axis). A two-curve pattern was frequently encountered in EC at a similar occurrence with SH and AH, indicating a heterogeneous population of cells regarding the number of signals per nucleus.

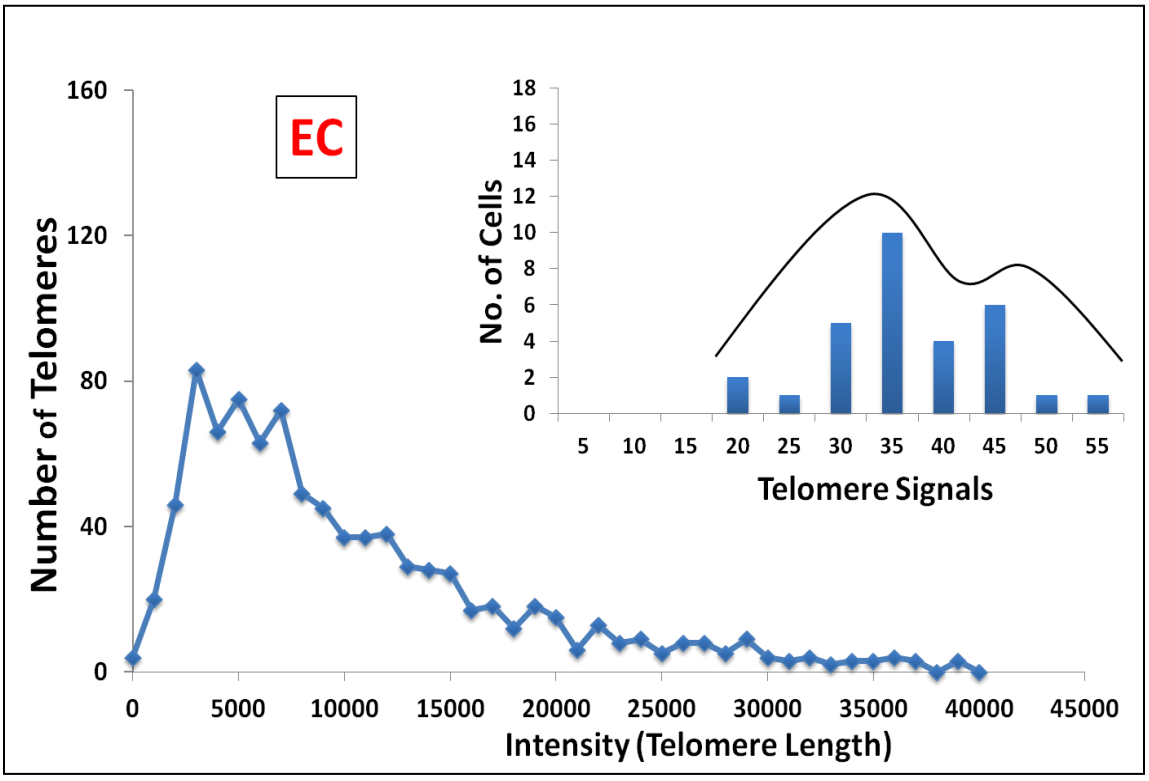

Fig. 13 Telomere Length Distribution

The graph illustrates 4 intensity groups (<6,000; 6,000-10,000; 10,000-20,000; >20,000) corresponding to the telomere length distribution in WT, SH, AH and EC and summary of results

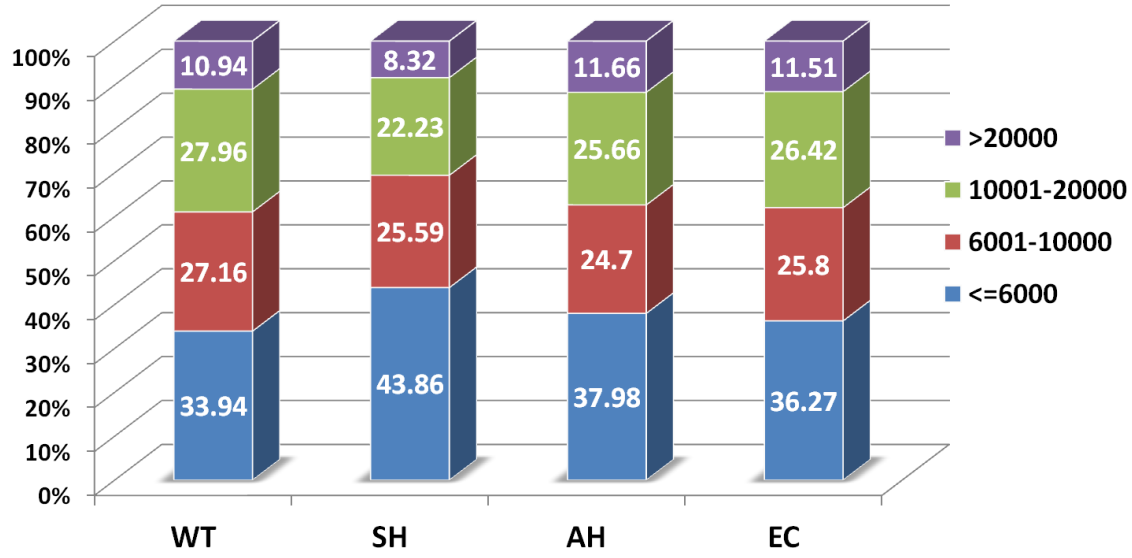

Intensity	Length	WT	SH	AH	EC	Significance	p value	
<=6000	Short Telomeres	33.94	**43.86**	37.98	36.27	**SH** vs WT	p=0.014	**SH ↑**
6001-10000	Medium Size Telomeres	27.16	25.59	**24.7**	25.8	**AH** vs WT	p=0.001	**AH↓**
10001-20000	Medium Size Telomeres	27.96	**22.23**	25.66	26.42	**SH** vs WT	p=0.005	**SH↓**
>20000	Long Telomeres	10.94	**8.32**	11.66	11.51	**SH** vs AH and EC	p=0.037; p=0.045	**SH↓**

5. Number of Telomeres

The total number of telomere signals detected in each sample was assessed after image deconvolution by using the Teloview software (Fig. 8). A number of 30 individual nuclei were analyzed for each animal and histo-pathological category. Next, the average number of telomeres in nuclei from each histo-pathological category was determined for all animals combined and compared to the telomere numbers of other pathologies. There were no significant differences among the four categories: WT, SH, AH and EC (Fig. 14)

Fig. 14 The average Number of Telomeres

The figure illustrates the average number of telomeres in WT, SH, AH and EC (per 30 nuclei). We analyzed a total number of 28 samples from WT mice and 48 samples from Pten heterozygous mice: 8 samples with SH pathology, 22 samples with AH pathology and 18 samples with EC pathology. No significant differences were observed.

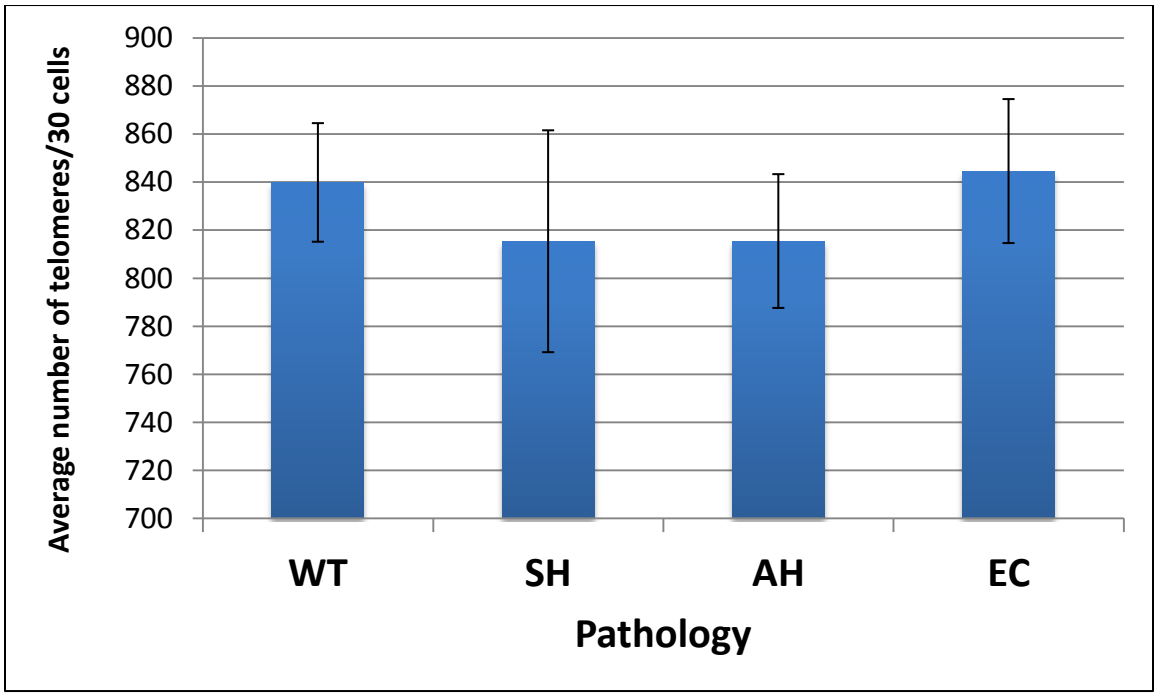

6. The 3D Telomere Distribution during the Cell Cycle

The space occupied by telomeres inside the nucleus can be defined by three axes: a, b and c, with a and b having the same length (spheroid). Previous data demonstrated that during the cell cycle the a/c ratio changes with only the c axis varying in length [127]. The a/c ratio is higher in proliferative cells when telomeres align at the center of the cell forming a disk (cells become more elongated). There were no significant differences in a/c ratio values in WT, SH, AH and EC (Fig. 15).

Fig. 15 3D Telomere Distribution during the Cell Cycle in WT, SH, AH and EC

This figure illustrates the a/c ratio, an indicator of the spatial placement of telomere signals inside the calculated nuclear volume; when the cell is more flat, this ratio increases. The differences among WT, SH, AH and EC were not significant.

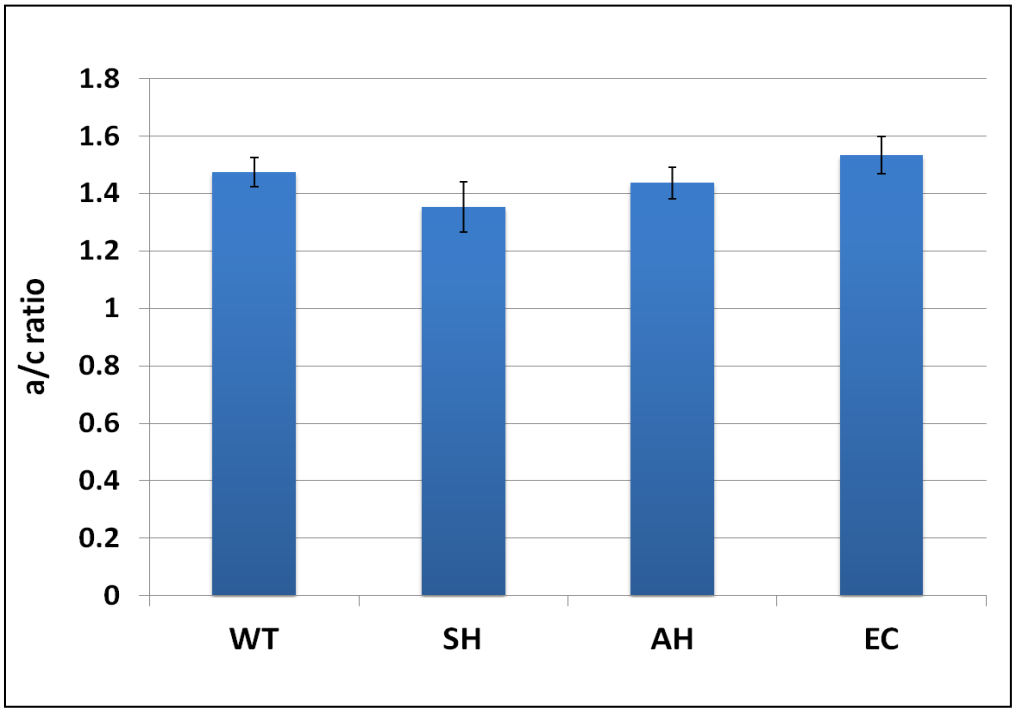

7. Telomere Aggregates

Telomere aggregates represent regions of associated telomere signals that cannot be resolved as separate objects by the normal 200 nm resolution limit. Thus, telomere aggregates may be the result of telomeres fused together or the effect of close proximity of neighboring telomeres. Telomere aggregates were identified in cancer cells and are an indicator of genomic instability [127, 132]. The 3D telomere architecture of the reconstructed images showed a significantly higher number of telomere aggregates in AH and EC compared to the WT and to the SH categories (Fig. 16). The number of telomere aggregates between WT and SH were indistinguishable (Fig.16).

Fig. 16 Telomere Aggregates in WT, SH, AH and EC

This graph illustrates the average number of telomere aggregates per nucleus calculated for a total number of 28 samples from WT mice, 8 samples with SH pathology, 22 samples with AH pathology and 18 samples with EC pathology from Pten heterozygous mice. The number of aggregates were found to be significantly higher in AH (p=0.0071) and EC (p=0.0002) compared to WT and SH.

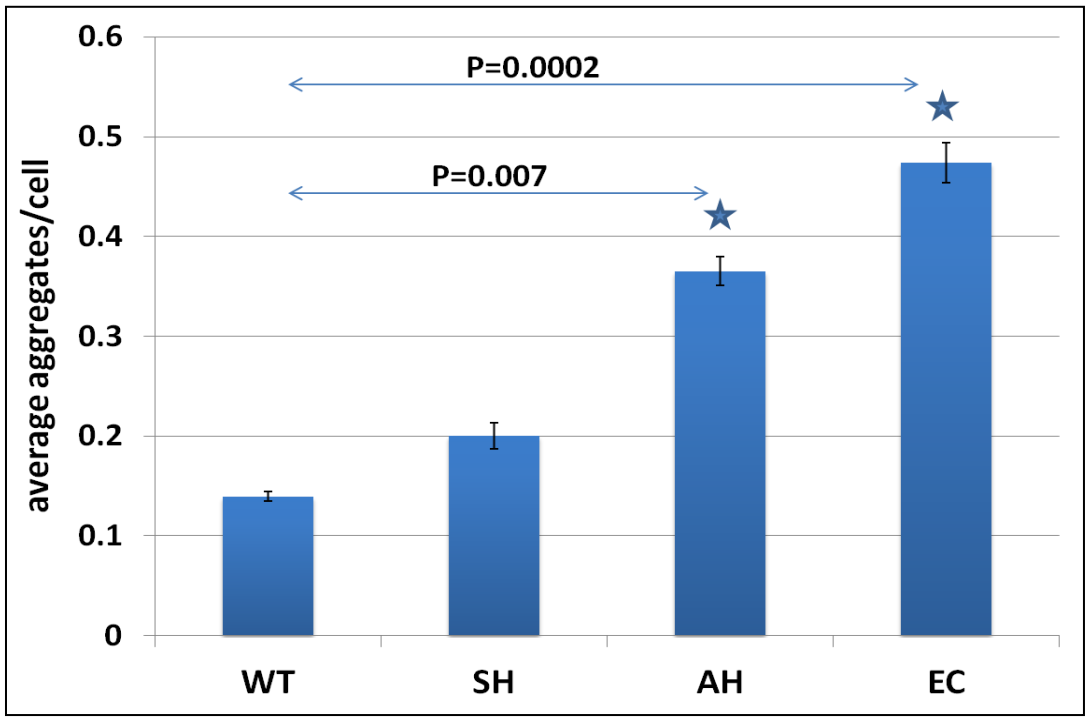

8. Summary of Telomere Results

a) We detected no age-related differences in telomere length in WT glandular epithelial cells.

b) The average number of telomeres per nucleus was not different between genotypes.

c) The spatial distribution of telomeric signals within the 3D nucleus (a/c ratio) was not different.

d) SH glandular epithelial cells displayed a higher number of short telomeres (< 6,000 intensity) and a lower number of telomeres in the 10,000 – 20,000 intensity group compared to WT cells.

e) SH pathology differed from AH and EC pathology; epithelial cells in SH glands had a higher number of short telomeres (< 6,000 intensity) and a lower number of telomeres in the >20,000 intensity group.

f) The AH pathology showed similar changes to EC in telomere intensity distribution, except for a lower number of telomeres in the 6,000 – 10,000 intensity group.

g) WT nuclei showed a single-curve distribution of telomere numbers over all analyzed nuclei per slide.

h) In contrast, a two-curved pattern was frequently detected in all Pten heterozygous pathologies.

i) An increase in telomere aggregates was observed in AH and EC when compared to WT and SH.

Table 2 **Summary of Telomere Results**

Pathology	WT (PTEN +/+)	SH (PTEN +/-)	AH (PTEN +/-)	EC (PTEN +/-)
Telomere Length Distribution	no difference	**↑ Short Telomeres ↓Medium Telomeres ↓Long Telomeres**	**↓Medium Telomeres**	no difference
Telomere Signal Distribution	one curve/ population	**two curves/ populations**	**two curves/ populations**	**two curves/ populations**
Telomere Distribution in the Nuclear Space	no difference	no difference	no difference	no difference
Telomere Aggregates	no difference	no difference	**↑ Telomere Aggregates**	**↑ Telomere Aggregates**
Average Number of Telomere Signals/ Nucleus	no difference	no difference	no difference	no difference

Chapter IV: DISCUSSION

Our work brings together an endometrial cancer mouse model and a new method for investigating the 3D telomere architectural changes inside the interphase nucleus during the development of endometrial malignancy.

Pten heterozygous mice develop endometrial cancer in a multistep process similar to the one seen in human type-I endometrial cancer. Glandular simple hyperplastic lesions progress to atypical forms of hyperplasia and finally transform into endometrial carcinoma. For research considerations we focused on the three main pathology stages: SH, AH and EC. Our question was: do changes in the nuclear 3D telomere architecture precede the development of carcinoma and if so, can there be detected prior to morphological evidence for endometrial carcinoma.

Despite the fact that the mouse estrous cycle is shorter, (around 4 days) and has different stages compared to the human cycle [159], the mouse offers numerous benefits for research in endometrial cancer. All animals have the same genetic background and consequently there is less phenotypic variation; WT mice are available from the same genetic background as an EC mouse model. Moreover, any medication that can influence endometrial physiology and hormonal state is excluded. Also, intermediate stages of carcinoma development can be more easily monitored.

Recent developments in microscopy combined with specific fluorescent techniques and the use of custom designed software allows us to investigate the 3D architecture of telomeres inside the cell nucleus [131]. Previous studies have improved the methods for investigating the 3D telomere architecture in the interphase nucleus, thus eliminating

the necessity of using metaphase spreads and greatly expanded the areas and types of research materials that can be investigated [131, 132, 160].

Our study focused on the 3D telomere architectural changes during endometrial carcinoma development. The semi-automated method used for the investigation of telomere architecture by 3D FISH benefits from the ability to consider clearly diagnosed pathology for in-situ analysis of archived tissues. Therefore, nuclei are investigated in their “natural” in-situ situation without provoking alterations potentially induced by isolating primary cells. In order to avoid bias in our 3D FISH experiments, 30 glandular cells from each considered sample were selected from the whole glandular cell population by randomizing the sample for statistical analysis. Clear rules were designed prior to the quantitative assessment. Criteria for rejecting a cell included an evaluation based on qualitative DNA counter staining (DAPI) and not on quantitative telomeric signals. Only the cells that appeared very fragmented or the cells overlapping other cells were excluded. This way, we analyzed a representative number of nuclei for each histology.

The 3D analysis of telomere organization inside the nuclei of endometrial glandular epithelial cells during carcinoma development revealed significant changes in all steps of malignant transformation. Several parameters were measured in order to characterize the 3D telomere architecture: telomere length and telomere signals distribution, telomere number, spatial distribution of telomeres inside the nucleus and formation of telomere aggregates**.**

1. Telomere length

Telomere shortening is not only specific to established cancer, but also occurs at an early, pre -invasive stage of cancer development [161, 162].

In our experiments, we found that SH lesions showed the highest number of short telomeres when compared to WT in contrast to AH and EC where the telomere length was similar to WT suggesting that there is a stabilization process against telomere attrition that cancer cells may acquire**.** Furthermore, the possible expression of active constitutive telomerase characteristic for the proliferative endometrial glandular cells can contribute to the stabilization of the telomere length once the malignancy progresses.

Previously, significant telomere shortening has been demonstrated to be an early event in human epithelial cancer development, such as those from prostate, pancreas, bladder, large intestine, esophagus, oral cavity or uterine cervix by using telomere-FISH techniques on histological specimens [161, 163, 164]. Short telomeres have also been described in breast ductal carcinoma in situ and in normal breast secretory cells. Interestingly these cells are highly proliferative under hormonal control and are the most susceptible to develop cancer.

We did not measure telomere changes in the surrounding stromal cells that had a normal histology and that may have an additional role in the carcinogenesis of this complex tissue. Recent experiments with isolated fractions of epithelial and stromal cells demonstrated different effects of estrogen treatment after biallelic Pten deletion

[76]. In contrast to epithelial cells, AKT was activated in stromal cells without requiring Pten loss [76]. PTEN inactivation may play a critical role in the regulation of telomere function in precancerous endometrial glands. Knock-down of wild-type PTEN in isolated epithelial endometrial cells and the detection of telomere 3D distribution changes may offer a more controlled model to investigate a possible functional correlation. Furthermore, re-introduction of PTEN in cancer epithelial endometrial cells followed by the telomere analysis could result in interesting observations regarding a potential effect of reversed telomere stabilization. PTEN may directly or indirectly interact with telomeric proteins and the loss of PTEN may be potentially involved in telomere dysfunction, although there is currently no experimental evidence for this.

Overall, our observations are in agreement with previous studies and suggest that telomere length shortening is one of the earliest genetic alterations involved in the multistep process of malignant transformation.

The majority of somatic cells have a protective mechanism against excessive shortening of telomeres, and consequently against chromosome instability and cancer development by limiting cell growth when telomere length has shortened beyond a critical point [116, 165, 166]. This event, when the shortening of the telomeres are inducing DNA damage checkpoints, is called “replicative senescence” [167, 168]. When these checkpoints are malfunctioning, cells continue to divide and to shorten their telomeres until another critical point called” telomere crisis” occurs [168]. Beyond this point cells become “immortal” and can continue to grow only if telomerase or

alternative mechanisms to maintain telomeres (ALT) are activated [169-171].

By using methods of mRNA detection, it was shown that in contrast to other human tissues, normal endometrial tissue expresses considerable telomerase activity in the glandular epithelial cells and this expression is dependent on the menstrual cycle [172, 173] [173, 174]. Cell proliferation is associated with telomerase expression and high levels of telomerase were detected also in human endometrial cancers [175-179] and in endometriosis [180]. Endometrial hyperplasia and endometrial cancer were demonstrated to have more stable telomere lengths that were maintained by constitutive telomerase expression. This contrast the situation observed in cervical, bladder, esophageal, gastric, head and neck, ovarian or renal cancers where the shortening of telomeres, measured by Southern blotting technique, was significant due to the lack of telomerase [181, 182]. Estrogen was shown to upregulate telomerase expression in the macacque [183]. Previously, it was shown that PTEN suppresses telomerase activity, and its loss possibly promotes malignant transformation of the endometrium displaying higher telomerase levels [184]. Loss of PTEN results in AKT phosphorylation and subsequent E2-independent activation of ER-alpha [73]. Although the level of telomerase activity has not been described in our Pten heterozygous mouse model, this mechanism may possibly aid in stabilizing the cancer genome in EC. One study found telomere length deregulation (shortening or lengthening) in 73.9% cases of endometrial cancer but the mean telomere length was not significantly changed [185]. In another study where “telomere chromogenic in situ hybridization” was used on epithelial and stromal (used as control) cells from archival human endometrial tumour

samples, initiation of EC type I was not associated with a significant number of critically short telomeres [186].

2. Total number of telomeres:

Aneuploidy (abnormal chromosome number) is a frequent occurrence in most human carcinomas [187], but it is unusual in endometrioid cancer when analyzed by flow cytometry [188]. According to our observations there were no significant differences between the average telomere number in endometrial glandular cells of control mice and the cells of Pten heterozygous mice with SH, AH or EC pathology. In order to further study a possible pattern of the variation in number of telomere signals in different clonal subpopulations of endometrial glandular cells we grouped them in different bins. More or less surprisingly, we frequently observed a heterogeneous population of cells in all Pten heterozygous mice when compared to WT controls. We found this pattern in all pathological categories including simple hyperplasia, atypical hyperplasia and carcinoma. This fact suggests a possible competitive clonal selection process that occurs early during the malignant transformation of the endometrial tissue, but may also prevail during late stages of EC. The average number of telomere signals detected in each cell does not consider the change in 3D telomere distribution profile or the change in telomere length.

3. Spatial distribution of telomeres in the 3D nucleus

Spatial positioning of chromosomes inside the nucleus during interphase was described to be non-random in mouse normal and cancer tissue [189]. The so called

"Chromosome territories" (CTs) represent an important characteristic of 3D nuclear architecture dynamics during diverse cellular functions [190]. Telomere 3D placements during cell cycle progression or during malignant transformation are an indicator of these nuclear architectural changes [129]. Thus, another parameter tested in the present study was the spatial distribution of telomeres defined by the a/c ratio. Telomeres are dynamically organized inside the nucleus and they can be characterized in different normal or transformed tissues, at different cell cycle points [127, 191, 192]. In normal lymphocytes, the organization of telomeres changes from the G0/G1 and S phases of the cell cycle when they are distributed throughout the entire nuclear volume to the G2 phase when they align in the center of the nucleus forming a telomere disk [127]. Therefore, a more flattened volume occupied by telomeres can be an indicator of a high cellular proliferation rate.

The a/c ratio in our mouse model endometrial glandular cells did not highlight any significant differences among WT, SH, AH and EC cells. The initial high turnover rate of endometrial glands in normal endometrium may be similar to the increased proliferation specific to cancer cells as demonstrated by the high expression of Ki-67 marker in human proliferative endometrium and endometrioid carcinoma [193].

4. Telomere aggregates

Formation of telomere aggregates is considered as a hallmark of cancer [132]. Quantitative analysis of the telomere aggregates confirmed a significantly increased number in AH and EC compared to WT and SH suggesting that telomere aggregate

formation represents a relatively late pre-cancerous event in malignant transformation of the endometrium. Telomere aggregates correspond to neighbouring telomere signals that cannot be resolved using the normal 200 nm resolution limit and may be the result of telomere end to end fusion as a consequence of telomere dysfunction or the effect of telomeres in close proximity. The latter would suggest that these telomeres have changed their spatial distribution. The "telomere-driven genome-instability" can result due to the close proximity of telomere territories that increases the risk of recombination especially in subtelomeric regions [191, 194]. Formation of telomere aggregates in cancer cells has been previously described in primary head and neck cancer, primary mouse plasmocytoma, human neuroblastoma, colon carcinoma cell lines [127, 132], human Burkitt lymphoma, glioblastoma [195], Hodgkin cells [196] and Reed-Sternberg cells [197].

The functional implications of nuclear architecture dynamics during normal and pathological development are not well understood. Different species or different cell types have similarities and differences in 3D nuclear organization of the nucleus that needs to be clarified in the future [198].

5. Conclusions

Endometrial glands of Pten heterozygous mice undergo histopathological changes, similar to EC process in humans, that modify the architecture of the glands in a multistep process ranging from simple hyperplasia (SH) to atypical hyperplasia (AH) and endometrial carcinoma (EC). PTEN protein expression in uterine glandular cells is

gradually diminished from SH to AH and EC lesions when the remaining PTEN allele is inactivated during carcinoma development.

Our data suggest that telomere dysfunction in Pten heterozygous mice in endometrial SH lesions starts prior to loss of PTEN protein expression. The more frequent appearance of short telomere signals and of two populations of cells with different telomere profiles in SH indicates the early onset of telomere dysfunction before PTEN loss.

We conclude that an increased number of shorter telomeres in SH is the earliest marker of structural telomere changes during EC development which precedes the loss of PTEN protein expression in more progressive glandular lesions followed by telomere aggregate formation in AH as an indicator for future cancer development. Also the high incidence of different subpopulations of glandular cells indicated by the heterogeneity in telomere signal bins present in SH, AH and EC suggest that telomere dysfunction is initiated very early in morphologically non-malignant endometrial tissue.

New methods are needed to better evaluate the risk of malignant transformation of precursor lesions and to decipher the mechanism of this transformation. Our work showed that the 3D telomere architecture has a specific signature that indicates early telomere dysfunction predictive for malignant transformation of endometrial tissue. Telomere shortening in the early phase of hyperplastic lesions of the endometrium along with the variation in telomere signal distribution in various cells of the same tissue

can provide indications of possible malignant evolution. Telomeres are dynamic structures occupying specific positions in the spatial nuclear volume.

More recently, new improvements in the 3D analysis of telomere profiles in interphase nuclei based on 3D-FISH were developed in Dr. Mai's lab. Using an automated scanner and specific software TeloScan, it is now possible to analyze more than 10 000 cells /hr and detect tumor cells in large samples. This method can assist in the detection of minimal residual disease and improve diagnosis and treatment management in different cancers [199].

By using quantitative 3D-telomere FISH, molecular imaging and analysis techniques applied to endometrial tissue, we demonstrated for the first time that 3D telomere architecture in glandular endometrial cells changes in early stages of simple hyperplasia before more morphologically advanced atypical hyperplasic lesions appear as endometrial pre-cancer. In future, this method may be translated into clinical use for the screening of endometrial hyperplastic lesions in order to predict potential malignant transformation.

REFERENCES

1. Jemal, A., et al., *Cancer statistics, 2010.* CA Cancer J Clin. **60**(5): p. 277-300.
2. Okuda, T., et al., *Genetics of endometrial cancers.* Obstet Gynecol Int. **2010**: p. 984013.
3. Hecht, J.L. and G.L. Mutter, *Molecular and pathologic aspects of endometrial carcinogenesis.* J Clin Oncol, 2006. **24**(29): p. 4783-91.
4. Doll, A., et al., *Novel molecular profiles of endometrial cancer-new light through old windows.* J Steroid Biochem Mol Biol, 2008. **108**(3-5): p. 221-9.
5. Koul, A., et al., *Distinct sets of gene alterations in endometrial carcinoma implicate alternate modes of tumorigenesis.* Cancer, 2002. **94**(9): p. 2369-79.
6. Lacey, J.V., Jr., et al., *Risk of subsequent endometrial carcinoma associated with endometrial intraepithelial neoplasia classification of endometrial biopsies.* Cancer, 2008. **113**(8): p. 2073-81.
7. Lacey, J.V., Jr., et al., *Absolute risk of endometrial carcinoma during 20-year follow-up among women with endometrial hyperplasia.* J Clin Oncol. **28**(5): p. 788-92.
8. Lacey, J.V., Jr. and V.M. Chia, *Endometrial hyperplasia and the risk of progression to carcinoma.* Maturitas, 2009. **63**(1): p. 39-44.
9. Di Cristofano, A., et al., *Pten is essential for embryonic development and tumour suppression.* Nat Genet, 1998. **19**(4): p. 348-55.
10. Podsypanina, K., et al., *Mutation of Pten/Mmac1 in mice causes neoplasia in multiple organ systems.* Proc Natl Acad Sci U S A, 1999. **96**(4): p. 1563-8.
11. Suzuki, A., et al., *High cancer susceptibility and embryonic lethality associated with mutation of the PTEN tumor suppressor gene in mice.* Curr Biol, 1998. **8**(21): p. 1169-78.
12. Gray, C.A., et al., *Developmental biology of uterine glands.* Biol Reprod, 2001. **65**(5): p. 1311-23.
13. Fazleabas, A.T. and Z. Strakova, *Endometrial function: cell specific changes in the uterine environment.* Mol Cell Endocrinol, 2002. **186**(2): p. 143-7.
14. Willing, C., et al., *Estrogen-independent actions of environmentally relevant AhR-agonists in human endometrial epithelial cells.* Mol Hum Reprod. **17**(2): p. 115-26.
15. Jabbour, H.N., et al., *Endocrine regulation of menstruation.* Endocr Rev, 2006. **27**(1): p. 17-46.
16. Lecce, G., et al., *Presence of estrogen receptor beta in the human endometrium through the cycle: expression in glandular, stromal, and vascular cells.* J Clin Endocrinol Metab, 2001. **86**(3): p. 1379-86.
17. Kastner, P., et al., *Two distinct estrogen-regulated promoters generate transcripts encoding the two functionally different human progesterone receptor forms A and B.* EMBO J, 1990. **9**(5): p. 1603-14.
18. Critchley, H.O., et al., *Estrogen receptor beta, but not estrogen receptor alpha, is present in the vascular endothelium of the human and nonhuman primate endometrium.* J Clin Endocrinol Metab, 2001. **86**(3): p. 1370-8.
19. Seppala, M. and A. Tiitinen, *Endometrial responses to corpus luteum products in cycles with induced ovulation: theoretical and practical considerations.* Hum Reprod, 1995. **10 Suppl 2**: p. 67-76.
20. Chauchereau, A., J.F. Savouret, and E. Milgrom, *Control of biosynthesis and post-transcriptional modification of the progesterone receptor.* Biol Reprod, 1992. **46**(2): p. 174-7.

21. Dockery, P. and A.W. Rogers, *The effects of steroids on the fine structure of the endometrium.* Baillieres Clin Obstet Gynaecol, 1989. **3**(2): p. 227-48.
22. Gosden, R.G. and E.B. James, *Menopause*, in *Encyclopedia of Gerontology*. 2007, Elsevier: New York. p. 151-159.
23. Hale, G.E., C.L. Hughes, and J.M. Cline, *Endometrial cancer: hormonal factors, the perimenopausal "window of risk," and isoflavones.* J Clin Endocrinol Metab, 2002. **87**(1): p. 3-15.
24. Kurman, R.J., P.F. Kaminski, and H.J. Norris, *The behavior of endometrial hyperplasia. A long-term study of "untreated" hyperplasia in 170 patients.* Cancer, 1985. **56**(2): p. 403-12.
25. Horn, L.C., et al., *Histopathology of endometrial hyperplasia and endometrial carcinoma: an update.* Ann Diagn Pathol, 2007. **11**(4): p. 297-311.
26. Jarboe, E.A. and G.L. Mutter, *Endometrial intraepithelial neoplasia.* Semin Diagn Pathol. **27**(4): p. 215-25.
27. Zaino, R.J., et al., *The prognostic value of nuclear versus architectural grading in endometrial adenocarcinoma: a Gynecologic Oncology Group study.* Int J Gynecol Pathol, 1994. **13**(1): p. 29-36.
28. Mutter, G.L., *Histopathology of genetically defined endometrial precancers.* Int J Gynecol Pathol, 2000. **19**(4): p. 301-9.
29. Potischman, N., et al., *Case-control study of endogenous steroid hormones and endometrial cancer.* J Natl Cancer Inst, 1996. **88**(16): p. 1127-35.
30. Ito, K., et al., *Inhibition of estrogen actions in human gynecological malignancies: New aspects of endocrine therapy for endometrial cancer and ovarian cancer.* Mol Cell Endocrinol.
31. Persson, I., *Estrogens in the causation of breast, endometrial and ovarian cancers - evidence and hypotheses from epidemiological findings.* J Steroid Biochem Mol Biol, 2000. **74**(5): p. 357-64.
32. Bokhman, J.V., *Two pathogenetic types of endometrial carcinoma.* Gynecol Oncol, 1983. **15**(1): p. 10-7.
33. Sherman, M.E., *Theories of endometrial carcinogenesis: a multidisciplinary approach.* Mod Pathol, 2000. **13**(3): p. 295-308.
34. Dobrzycka, B. and S.J. Terlikowski, *Biomarkers as prognostic factors in endometrial cancer.* Folia Histochem Cytobiol. **48**(3): p. 319-22.
35. Prat, J., *Prognostic parameters of endometrial carcinoma.* Hum Pathol, 2004. **35**(6): p. 649-62.
36. Lax, S.F. and R.J. Kurman, *A dualistic model for endometrial carcinogenesis based on immunohistochemical and molecular genetic analyses.* Verh Dtsch Ges Pathol, 1997. **81**: p. 228-32.
37. Marsden, D.E. and N.F. Hacker, *Optimal management of endometrial hyperplasia.* Best Pract Res Clin Obstet Gynaecol, 2001. **15**(3): p. 393-405.
38. Sivridis, E. and A. Giatromanolaki, *The endometrial hyperplasias revisited.* Virchows Arch, 2008. **453**(3): p. 223-31.
39. Mazur, M.T., *Endometrial hyperplasia/adenocarcinoma. a conventional approach.* Ann Diagn Pathol, 2005. **9**(3): p. 174-81.
40. Bergeron, C., et al., *A multicentric European study testing the reproducibility of the WHO classification of endometrial hyperplasia with a proposal of a simplified working classification for biopsy and curettage specimens.* Am J Surg Pathol, 1999. **23**(9): p. 1102-8.

41. Hecht, J.L., et al., *Prediction of endometrial carcinoma by subjective endometrial intraepithelial neoplasia diagnosis.* Mod Pathol, 2005. **18**(3): p. 324-30.
42. Randall, T.C. and R.J. Kurman, *Progestin treatment of atypical hyperplasia and well-differentiated carcinoma of the endometrium in women under age 40.* Obstet Gynecol, 1997. **90**(3): p. 434-40.
43. Latta, E. and W.B. Chapman, *PTEN mutations and evolving concepts in endometrial neoplasia.* Curr Opin Obstet Gynecol, 2002. **14**(1): p. 59-65.
44. Mutter, G.L., et al., *Altered PTEN expression as a diagnostic marker for the earliest endometrial precancers.* J Natl Cancer Inst, 2000. **92**(11): p. 924-30.
45. MacDonald, N.D., et al., *Frequency and prognostic impact of microsatellite instability in a large population-based study of endometrial carcinomas.* Cancer Res, 2000. **60**(6): p. 1750-2.
46. Sasaki, H., et al., *Mutation of the Ki-ras protooncogene in human endometrial hyperplasia and carcinoma.* Cancer Res, 1993. **53**(8): p. 1906-10.
47. Palacios, J., et al., *Beta- and gamma-catenin expression in endometrial carcinoma. Relationship with clinicopathological features and microsatellite instability.* Virchows Arch, 2001. **438**(5): p. 464-9.
48. Lax, S.F., et al., *The frequency of p53, K-ras mutations, and microsatellite instability differs in uterine endometrioid and serous carcinoma: evidence of distinct molecular genetic pathways.* Cancer, 2000. **88**(4): p. 814-24.
49. Trope, C., G.B. Kristensen, and V.M. Abeler, *Clear-cell and papillary serous cancer: treatment options.* Best Pract Res Clin Obstet Gynaecol, 2001. **15**(3): p. 433-46.
50. Li, J., et al., *PTEN, a putative protein tyrosine phosphatase gene mutated in human brain, breast, and prostate cancer.* Science, 1997. **275**(5308): p. 1943-7.
51. Li, D.M. and H. Sun, *TEP1, encoded by a candidate tumor suppressor locus, is a novel protein tyrosine phosphatase regulated by transforming growth factor beta.* Cancer Res, 1997. **57**(11): p. 2124-9.
52. Steck, P.A., et al., *Identification of a candidate tumour suppressor gene, MMAC1, at chromosome 10q23.3 that is mutated in multiple advanced cancers.* Nat Genet, 1997. **15**(4): p. 356-62.
53. Wang, S.I., et al., *Somatic mutations of PTEN in glioblastoma multiforme.* Cancer Res, 1997. **57**(19): p. 4183-6.
54. Tashiro, H., et al., *Mutations in PTEN are frequent in endometrial carcinoma but rare in other common gynecological malignancies.* Cancer Res, 1997. **57**(18): p. 3935-40.
55. Cairns, P., et al., *Frequent inactivation of PTEN/MMAC1 in primary prostate cancer.* Cancer Res, 1997. **57**(22): p. 4997-5000.
56. Bonneau, D. and M. Longy, *Mutations of the human PTEN gene.* Hum Mutat, 2000. **16**(2): p. 109-22.
57. Stambolic, V., et al., *High incidence of breast and endometrial neoplasia resembling human Cowden syndrome in pten+/- mice.* Cancer Res, 2000. **60**(13): p. 3605-11.
58. Di Cristofano, A. and P.P. Pandolfi, *The multiple roles of PTEN in tumor suppression.* Cell, 2000. **100**(4): p. 387-90.
59. Chow, L.M. and S.J. Baker, *PTEN function in normal and neoplastic growth.* Cancer Lett, 2006. **241**(2): p. 184-96.
60. Li, L. and A.H. Ross, *Why is PTEN an important tumor suppressor?* J Cell Biochem, 2007. **102**(6): p. 1368-74.
61. Kanamori, Y., et al., *Correlation between loss of PTEN expression and Akt phosphorylation in endometrial carcinoma.* Clin Cancer Res, 2001. **7**(4): p. 892-5.

62. Bartek, J. and J. Lukas, *Chk1 and Chk2 kinases in checkpoint control and cancer.* Cancer Cell, 2003. **3**(5): p. 421-9.
63. Puc, J., et al., *Lack of PTEN sequesters CHK1 and initiates genetic instability.* Cancer Cell, 2005. **7**(2): p. 193-204.
64. Sorensen, C.S., et al., *The cell-cycle checkpoint kinase Chk1 is required for mammalian homologous recombination repair.* Nat Cell Biol, 2005. **7**(2): p. 195-201.
65. Shen, W.H., et al., *Essential role for nuclear PTEN in maintaining chromosomal integrity.* Cell, 2007. **128**(1): p. 157-70.
66. Lax, S.F., *Molecular genetic pathways in various types of endometrial carcinoma: from a phenotypical to a molecular-based classification.* Virchows Arch, 2004. **444**(3): p. 213-23.
67. Rasheed, B.K., et al., *PTEN gene mutations are seen in high-grade but not in low-grade gliomas.* Cancer Res, 1997. **57**(19): p. 4187-90.
68. Whang, Y.E., et al., *Inactivation of the tumor suppressor PTEN/MMAC1 in advanced human prostate cancer through loss of expression.* Proc Natl Acad Sci U S A, 1998. **95**(9): p. 5246-50.
69. Levine, R.L., et al., *PTEN mutations and microsatellite instability in complex atypical hyperplasia, a precursor lesion to uterine endometrioid carcinoma.* Cancer Res, 1998. **58**(15): p. 3254-8.
70. Mutter, G.L., et al., *Molecular identification of latent precancers in histologically normal endometrium.* Cancer Res, 2001. **61**(11): p. 4311-4.
71. Mutter, G.L., et al., *Changes in endometrial PTEN expression throughout the human menstrual cycle.* J Clin Endocrinol Metab, 2000. **85**(6): p. 2334-8.
72. Campbell, R.A., et al., *Phosphatidylinositol 3-kinase/AKT-mediated activation of estrogen receptor alpha: a new model for anti-estrogen resistance.* J Biol Chem, 2001. **276**(13): p. 9817-24.
73. Vilgelm, A., et al., *Akt-mediated phosphorylation and activation of estrogen receptor alpha is required for endometrial neoplastic transformation in Pten+/- mice.* Cancer Res, 2006. **66**(7): p. 3375-80.
74. Saito, F., et al., *Mutual contribution of Pten and estrogen to endometrial carcinogenesis in a PtenloxP/loxP mouse model.* Int J Gynecol Cancer, 2011. **21**(8): p. 1343-9.
75. Stoica, G.E., et al., *Effect of estradiol on estrogen receptor-alpha gene expression and activity can be modulated by the ErbB2/PI 3-K/Akt pathway.* Oncogene, 2003. **22**(39): p. 7998-8011.
76. Joshi, A. and L.H. Ellenson, *Adenovirus mediated homozygous endometrial epithelial Pten deletion results in aggressive endometrial carcinoma.* Exp Cell Res, 2011. **317**(11): p. 1580-9.
77. Blumenthal, G.M. and P.A. Dennis, *PTEN hamartoma tumor syndromes.* Eur J Hum Genet, 2008. **16**(11): p. 1289-300.
78. Gustafson, S., et al., *Cowden syndrome.* Semin Oncol, 2007. **34**(5): p. 428-34.
79. Ilyas, M. and I.P. Tomlinson, *Genetic pathways in colorectal cancer.* Histopathology, 1996. **28**(5): p. 389-99.
80. Nowell, P.C., *The clonal evolution of tumor cell populations.* Science, 1976. **194**(4260): p. 23-8.
81. Lengauer, C., K.W. Kinzler, and B. Vogelstein, *Genetic instabilities in human cancers.* Nature, 1998. **396**(6712): p. 643-9.
82. Fearon, E.R. and B. Vogelstein, *A genetic model for colorectal tumorigenesis.* Cell, 1990. **61**(5): p. 759-67.

83. Widschwendter, M., et al., *Epigenetic stem cell signature in cancer.* Nat Genet, 2007. **39**(2): p. 157-8.
84. Blackburn, E.H., *Switching and signaling at the telomere.* Cell, 2001. **106**(6): p. 661-73.
85. Chan, S.W. and E.H. Blackburn, *New ways not to make ends meet: telomerase, DNA damage proteins and heterochromatin.* Oncogene, 2002. **21**(4): p. 553-63.
86. de Lange, T., *Protection of mammalian telomeres.* Oncogene, 2002. **21**(4): p. 532-40.
87. Griffith, J.D., et al., *Mammalian telomeres end in a large duplex loop.* Cell, 1999. **97**(4): p. 503-14.
88. Greider, C.W. and E.H. Blackburn, *A telomeric sequence in the RNA of Tetrahymena telomerase required for telomere repeat synthesis.* Nature, 1989. **337**(6205): p. 331-7.
89. Olovnikov, A.M., *A theory of marginotomy. The incomplete copying of template margin in enzymic synthesis of polynucleotides and biological significance of the phenomenon.* J Theor Biol, 1973. **41**(1): p. 181-90.
90. Watson, J.D., *Origin of concatemeric T7 DNA.* Nat New Biol, 1972. **239**(94): p. 197-201.
91. Hayflick, L., *The Limited in Vitro Lifetime of Human Diploid Cell Strains.* Exp Cell Res, 1965. **37**: p. 614-36.
92. Harley, C.B., et al., *The telomere hypothesis of cellular aging.* Exp Gerontol, 1992. **27**(4): p. 375-82.
93. Greider, C.W., *Telomeres, telomerase and senescence.* Bioessays, 1990. **12**(8): p. 363-9.
94. Barnett, M.A., et al., *Telomere directed fragmentation of mammalian chromosomes.* Nucleic Acids Res, 1993. **21**(1): p. 27-36.
95. Campisi, J., *Cancer, aging and cellular senescence.* In Vivo, 2000. **14**(1): p. 183-8.
96. Nyberg, K.A., et al., *Toward maintaining the genome: DNA damage and replication checkpoints.* Annu Rev Genet, 2002. **36**: p. 617-56.
97. Martinez, P., et al., *Increased telomere fragility and fusions resulting from TRF1 deficiency lead to degenerative pathologies and increased cancer in mice.* Genes Dev, 2009. **23**(17): p. 2060-75.
98. de Lange, T., *Shelterin: the protein complex that shapes and safeguards human telomeres.* Genes Dev, 2005. **19**(18): p. 2100-10.
99. Palm, W. and T. de Lange, *How shelterin protects mammalian telomeres.* Annu Rev Genet, 2008. **42**: p. 301-34.
100. Broccoli, D., et al., *Human telomeres contain two distinct Myb-related proteins, TRF1 and TRF2.* Nat Genet, 1997. **17**(2): p. 231-5.
101. Yang, Q., Y.L. Zheng, and C.C. Harris, *POT1 and TRF2 cooperate to maintain telomeric integrity.* Mol Cell Biol, 2005. **25**(3): p. 1070-80.
102. Smogorzewska, A., et al., *Control of human telomere length by TRF1 and TRF2.* Mol Cell Biol, 2000. **20**(5): p. 1659-68.
103. Murnane, J.P., *Telomeres and chromosome instability.* DNA Repair (Amst), 2006. **5**(9-10): p. 1082-92.
104. Denchi, E.L. and T. de Lange, *Protection of telomeres through independent control of ATM and ATR by TRF2 and POT1.* Nature, 2007. **448**(7157): p. 1068-71.
105. Loayza, D. and T. De Lange, *POT1 as a terminal transducer of TRF1 telomere length control.* Nature, 2003. **423**(6943): p. 1013-8.
106. Possemato, R., et al., *Suppression of hPOT1 in diploid human cells results in an hTERT-dependent alteration of telomere length dynamics.* Mol Cancer Res, 2008. **6**(10): p. 1582-93.
107. Xin, H., et al., *TPP1 is a homologue of ciliate TEBP-beta and interacts with POT1 to recruit telomerase.* Nature, 2007. **445**(7127): p. 559-62.

108. Hockemeyer, D., et al., *Telomere protection by mammalian Pot1 requires interaction with Tpp1.* Nat Struct Mol Biol, 2007. **14**(8): p. 754-61.
109. Liu, D., et al., *PTOP interacts with POT1 and regulates its localization to telomeres.* Nat Cell Biol, 2004. **6**(7): p. 673-80.
110. Takai, K.K., et al., *In vivo stoichiometry of shelterin components.* J Biol Chem, 2010. **285**(2): p. 1457-67.
111. Kim, S.H., et al., *TIN2 mediates functions of TRF2 at human telomeres.* J Biol Chem, 2004. **279**(42): p. 43799-804.
112. Li, B., S. Oestreich, and T. de Lange, *Identification of human Rap1: implications for telomere evolution.* Cell, 2000. **101**(5): p. 471-83.
113. Mai, S. and J.F. Mushinski, *c-Myc-induced genomic instability.* J Environ Pathol Toxicol Oncol, 2003. **22**(3): p. 179-99.
114. Pampalona, J., et al., *Whole chromosome loss is promoted by telomere dysfunction in primary cells.* Genes Chromosomes Cancer. **49**(4): p. 368-78.
115. McClintock, B., *The Stability of Broken Ends of Chromosomes in Zea Mays.* Genetics, 1941. **26**(2): p. 234-82.
116. Verdun, R.E. and J. Karlseder, *Replication and protection of telomeres.* Nature, 2007. **447**(7147): p. 924-31.
117. DePinho, R.A. and K. Polyak, *Cancer chromosomes in crisis.* Nat Genet, 2004. **36**(9): p. 932-4.
118. Csink, A.K. and S. Henikoff, *Genetic modification of heterochromatic association and nuclear organization in Drosophila.* Nature, 1996. **381**(6582): p. 529-31.
119. Brown, K.E., et al., *Association of transcriptionally silent genes with Ikaros complexes at centromeric heterochromatin.* Cell, 1997. **91**(6): p. 845-54.
120. Croft, J.A., et al., *Differences in the localization and morphology of chromosomes in the human nucleus.* J Cell Biol, 1999. **145**(6): p. 1119-31.
121. Chevret, E., E.V. Volpi, and D. Sheer, *Mini review: form and function in the human interphase chromosome.* Cytogenet Cell Genet, 2000. **90**(1-2): p. 13-21.
122. Verschure, P.J., et al., *Spatial relationship between transcription sites and chromosome territories.* J Cell Biol, 1999. **147**(1): p. 13-24.
123. Cremer, T., et al., *Chromosome territories, interchromatin domain compartment, and nuclear matrix: an integrated view of the functional nuclear architecture.* Crit Rev Eukaryot Gene Expr, 2000. **10**(2): p. 179-212.
124. Schneider, R. and R. Grosschedl, *Dynamics and interplay of nuclear architecture, genome organization, and gene expression.* Genes Dev, 2007. **21**(23): p. 3027-43.
125. Cremer, T., et al., *Role of chromosome territories in the functional compartmentalization of the cell nucleus.* Cold Spring Harb Symp Quant Biol, 1993. **58**: p. 777-92.
126. Dietzel, S., et al., *The 3D positioning of ANT2 and ANT3 genes within female X chromosome territories correlates with gene activity.* Exp Cell Res, 1999. **252**(2): p. 363-75.
127. Chuang, T.C., et al., *The three-dimensional organization of telomeres in the nucleus of mammalian cells.* BMC Biol, 2004. **2**: p. 12.
128. Mai, S. and Y. Garini, *Oncogenic remodeling of the three-dimensional organization of the interphase nucleus: c-Myc induces telomeric aggregates whose formation precedes chromosomal rearrangements.* Cell Cycle, 2005. **4**(10): p. 1327-31.
129. Mai, S., *Initiation of telomere-mediated chromosomal rearrangements in cancer.* J Cell Biochem. **109**(6): p. 1095-102.

130. Klonisch, T., et al., *Nuclear imaging in three dimensions: a unique tool in cancer research.* Ann Anat. **192**(5): p. 292-301.
131. Vermolen, B.J., et al., *Characterizing the three-dimensional organization of telomeres.* Cytometry A, 2005. **67**(2): p. 144-50.
132. Mai, S. and Y. Garini, *The significance of telomeric aggregates in the interphase nuclei of tumor cells.* J Cell Biochem, 2006. **97**(5): p. 904-15.
133. Köhler, A., *Ein neues Beleuchtungsverfahren für mikrophotographische Zwecke"*, in *Zeitschrift für wissenschaftliche Mikroskopie und für Mikroskopische Technik **10** (4): 433-440.*
. 1893.
134. *Zernike, F., Phase-contrast, a new method for microscopic observation of transparent objects. Part II*, in *Physica: 9, 974-986* 1942.
135. Geissinger, D., K. Sonstegard, and R. Sonstegard, *Nomarski differential interference contrast--fluorescence microscopy: a new technique designed to improve resolution in fluorescent specimen.* Mikroskopie, 1970. **24**(11): p. 321-6.
136. McNally, J.G., et al., *Three-dimensional imaging by deconvolution microscopy.* Methods, 1999. **19**(3): p. 373-85.
137. Sun, Y., et al., *An open-source deconvolution software package for 3-D quantitative fluorescence microscopy imaging.* J Microsc, 2009. **236**(3): p. 180-93.
138. Heintzmann, R. and G. Ficz, *Breaking the resolution limit in light microscopy.* Brief Funct Genomic Proteomic, 2006. **5**(4): p. 289-301.
139. Agard, D.A., et al., *Fluorescence microscopy in three dimensions.* Methods Cell Biol, 1989. **30**: p. 353-77.
140. Andrews, P.D., I.S. Harper, and J.R. Swedlow, *To 5D and beyond: quantitative fluorescence microscopy in the postgenomic era.* Traffic, 2002. **3**(1): p. 29-36.
141. Abbe, E., *Arch. f. Mikroskop. Anat.* ***9*** *- 413*. 1873.
142. Wolf, D.E., *The optics of microscope image formation.* Methods Cell Biol, 2003. **72**: p. 11-43.
143. Bahlmann, K., S. Jakobs, and S.W. Hell, *4Pi-confocal microscopy of live cells.* Ultramicroscopy, 2001. **87**(3): p. 155-64.
144. Qu, X., et al., *Nanometer-localized multiple single-molecule fluorescence microscopy.* Proc Natl Acad Sci U S A, 2004. **101**(31): p. 11298-303.
145. Carlton, P.M., *Three-dimensional structured illumination microscopy and its application to chromosome structure.* Chromosome Res, 2008. **16**(3): p. 351-65.
146. Smith, W.S.B.a.G.E., *Charge Coupled Semiconductor Devices.* ". *Bell Sys. Tech. J.* **49** (4): 587-593, 1970.
147. Hiraoka, Y., J.W. Sedat, and D.A. Agard, *The use of a charge-coupled device for quantitative optical microscopy of biological structures.* Science, 1987. **238**(4823): p. 36-41.
148. Aikens, R.S., D.A. Agard, and J.W. Sedat, *Solid-state imagers for microscopy.* Methods Cell Biol, 1989. **29**: p. 291-313.
149. Preza, C., et al., *Regularized linear method for reconstruction of three-dimensional microscopic objects from optical sections.* J Opt Soc Am A, 1992. **9**(2): p. 219-28.
150. Verveer, P.J., M.J. Gemkow, and T.M. Jovin, *A comparison of image restoration approaches applied to three-dimensional confocal and wide-field fluorescence microscopy.* J Microsc, 1999. **193**(1): p. 50-61.

151. Schaefer, L.H., D. Schuster, and H. Herz, *Generalized approach for accelerated maximum likelihood based image restoration applied to three-dimensional fluorescence microscopy.* J Microsc, 2001. **204**(Pt 2): p. 99-107.
152. Markham, J. and J.A. Conchello, *Parametric blind deconvolution: a robust method for the simultaneous estimation of image and blur.* J Opt Soc Am A Opt Image Sci Vis, 1999. **16**(10): p. 2377-91.
153. Raap, A.K., *Advances in fluorescence in situ hybridization.* Mutat Res, 1998. **400**(1-2): p. 287-98.
154. Bauman, J.G., et al., *A new method for fluorescence microscopical localization of specific DNA sequences by in situ hybridization of fluorochromelabelled RNA.* Exp Cell Res, 1980. **128**(2): p. 485-90.
155. Price, C.M., *Fluorescence in situ hybridization.* Blood Rev, 1993. **7**(2): p. 127-34.
156. Visser, A.E., et al., *Spatial distributions of early and late replicating chromatin in interphase chromosome territories.* Exp Cell Res, 1998. **243**(2): p. 398-407.
157. Solovei, I., et al., *Spatial preservation of nuclear chromatin architecture during three-dimensional fluorescence in situ hybridization (3D-FISH).* Exp Cell Res, 2002. **276**(1): p. 10-23.
158. Poon, T.C. and T. Kim, *Optical image recognition of three-dimensional objects.* Appl Opt, 1999. **38**(2): p. 370-81.
159. Nishimura, T., *The short estrous cycle of mice may influence the effect of BRCA1 mutations.* Med Hypotheses. **77**(3): p. 401-3.
160. Klonisch, T., et al., *Nuclear imaging in three dimensions: a unique tool in cancer research.* Ann Anat, 2010. **192**(5): p. 292-301.
161. Meeker, A.K., et al., *Telomere length abnormalities occur early in the initiation of epithelial carcinogenesis.* Clin Cancer Res, 2004. **10**(10): p. 3317-26.
162. Meeker, A.K., et al., *Telomere shortening occurs in subsets of normal breast epithelium as well as in situ and invasive carcinoma.* Am J Pathol, 2004. **164**(3): p. 925-35.
163. Meeker, A.K., et al., *Telomere shortening is an early somatic DNA alteration in human prostate tumorigenesis.* Cancer Res, 2002. **62**(22): p. 6405-9.
164. van Heek, N.T., et al., *Telomere shortening is nearly universal in pancreatic intraepithelial neoplasia.* Am J Pathol, 2002. **161**(5): p. 1541-7.
165. Hemann, M.T., et al., *The shortest telomere, not average telomere length, is critical for cell viability and chromosome stability.* Cell, 2001. **107**(1): p. 67-77.
166. Viscardi, V., et al., *Telomeres and DNA damage checkpoints.* Biochimie, 2005. **87**(7): p. 613-24.
167. Stewart, S.A., et al., *Erosion of the telomeric single-strand overhang at replicative senescence.* Nat Genet, 2003. **33**(4): p. 492-6.
168. Shay, J.W. and W.E. Wright, *Senescence and immortalization: role of telomeres and telomerase.* Carcinogenesis, 2005. **26**(5): p. 867-74.
169. Heaphy, C.M., et al., *Prevalence of the alternative lengthening of telomeres telomere maintenance mechanism in human cancer subtypes.* Am J Pathol, 2011. **179**(4): p. 1608-15.
170. Stewart, S.A., *Telomere maintenance and tumorigenesis: an "ALT"ernative road.* Curr Mol Med, 2005. **5**(2): p. 253-7.
171. Stewart, S.A., et al., *Telomerase contributes to tumorigenesis by a telomere length-independent mechanism.* Proc Natl Acad Sci U S A, 2002. **99**(20): p. 12606-11.
172. Kyo, S., et al., *Telomerase activity in human endometrium.* Cancer Res, 1997. **57**(4): p. 610-4.

173. Tanaka, M., et al., *Expression of telomerase activity in human endometrium is localized to epithelial glandular cells and regulated in a menstrual phase-dependent manner correlated with cell proliferation.* Am J Pathol, 1998. **153**(6): p. 1985-91.
174. Yokoyama, Y., et al., *Telomerase activity is found in the epithelial cells but not in the stromal cells in human endometrial cell culture.* Mol Hum Reprod, 1998. **4**(10): p. 985-9.
175. Greider, C.W., *Telomerase activity, cell proliferation, and cancer.* Proc Natl Acad Sci U S A, 1998. **95**(1): p. 90-2.
176. Oshita, T., N. Nagai, and K. Ohama, *Expression of telomerase reverse transcriptase mRNA and its quantitative analysis in human endometrial cancer.* Int J Oncol, 2000. **17**(6): p. 1225-30.
177. Lehner, R., et al., *Quantitative analysis of telomerase hTERT mRNA and telomerase activity in endometrioid adenocarcinoma and in normal endometrium.* Gynecol Oncol, 2002. **84**(1): p. 120-5.
178. Kyo, S., et al., *Human telomerase reverse transcriptase as a critical determinant of telomerase activity in normal and malignant endometrial tissues.* Int J Cancer, 1999. **80**(1): p. 60-3.
179. Bonatz, G., et al., *High telomerase activity is associated with cell cycle deregulation and rapid progression in endometrioid adenocarcinoma of the uterus.* Hum Pathol, 2001. **32**(6): p. 605-14.
180. Hapangama, D.K., et al., *Endometriosis is associated with aberrant endometrial expression of telomerase and increased telomere length.* Hum Reprod, 2008. **23**(7): p. 1511-9.
181. Maida, Y., et al., *Distinct telomere length regulation in premalignant cervical and endometrial lesions: implications for the roles of telomeres in uterine carcinogenesis.* J Pathol, 2006. **210**(2): p. 214-23.
182. Wentzensen, I.M., et al., *The association of telomere length and cancer: a meta-analysis.* Cancer Epidemiol Biomarkers Prev. **20**(6): p. 1238-50.
183. Vidal, J.D., et al., *Estrogen replacement therapy induces telomerase RNA expression in the macaque endometrium.* Fertil Steril, 2002. **77**(3): p. 601-8.
184. Zhou, C., et al., *The PTEN tumor suppressor inhibits telomerase activity in endometrial cancer cells by decreasing hTERT mRNA levels.* Gynecol Oncol, 2006. **101**(2): p. 305-10.
185. Wang, S.J., et al., *The relationship between telomere length and telomerase activity in gynecologic cancers.* Gynecol Oncol, 2002. **84**(1): p. 81-4.
186. Akbay, E.A., et al., *Differential roles of telomere attrition in type I and II endometrial carcinogenesis.* Am J Pathol, 2008. **173**(2): p. 536-44.
187. Jonsdottir, A.B., et al., *Tetraploidy in BRCA2 breast tumours.* Eur J Cancer, 2011.
188. Rosenberg, P., et al., *Flow cytometric measurements of DNA index and S-phase on paraffin-embedded early stage endometrial cancer: an important prognostic indicator.* Gynecol Oncol, 1989. **35**(1): p. 50-4.
189. Parada, L.A., et al., *Conservation of relative chromosome positioning in normal and cancer cells.* Curr Biol, 2002. **12**(19): p. 1692-7.
190. Cremer, T. and M. Cremer, *Chromosome territories.* Cold Spring Harb Perspect Biol, 2010. **2**(3): p. a003889.
191. De Vos, W.H., et al., *Controlled light exposure microscopy reveals dynamic telomere microterritories throughout the cell cycle.* Cytometry A, 2009. **75**(5): p. 428-39.
192. Gadji, M., et al., *Three-dimensional nuclear telomere architecture is associated with differential time to progression and overall survival in glioblastoma patients.* Neoplasia, 2010. **12**(2): p. 183-91.

193. Kosmas, K., et al., *Expression of ki-67 as proliferation biomarker in imprint smears of endometrial carcinoma.* Diagn Cytopathol, 2011.
194. Linardopoulou, E.V., et al., *Human subtelomeres are hot spots of interchromosomal recombination and segmental duplication.* Nature, 2005. **437**(7055): p. 94-100.
195. Gadji, M., et al., *Three-dimensional nuclear telomere architecture is associated with differential time to progression and overall survival in glioblastoma patients.* Neoplasia. **12**(2): p. 183-91.
196. Knecht, H., et al., *3D nuclear organization of telomeres in the Hodgkin cell lines U-HO1 and U-HO1-PTPN1: PTPN1 expression prevents the formation of very short telomeres including "t-stumps".* BMC Cell Biol. **11**: p. 99.
197. Knecht, H., et al., *3D structural and functional characterization of the transition from Hodgkin to Reed-Sternberg cells.* Ann Anat. **192**(5): p. 302-8.
198. Foster, H.A. and J.M. Bridger, *The genome and the nucleus: a marriage made by evolution. Genome organisation and nuclear architecture.* Chromosoma, 2005. **114**(4): p. 212-29.
199. Klewes, L., et al., *Novel automated three-dimensional genome scanning based on the nuclear architecture of telomeres.* Cytometry A. **79**(2): p. 159-66.